

# Diagonal Coset Approach to Topological Quantum Computation with Fibonacci Anyons

Lachezar S. Georgiev, Ludmil Hadjiivanov and Grigori Matein

*Institute for Nuclear Research and Nuclear Energy  
Bulgarian Academy of Sciences  
Tsarigradsko Chaussee 72, 1784 Sofia, BULGARIA*

---

## Abstract

We investigate a promising conformal field theory realization scheme for topological quantum computation based on the Fibonacci anyons, which are believed to be realized as quasi-particle excitations in the  $\mathbb{Z}_3$  parafermion fractional quantum Hall state in the second Landau level with filling factor  $\nu = 12/5$ . These anyons are non-Abelian and are known to be capable of universal topological quantum computation. The quantum information is encoded in the fusion channels of pairs of such non-Abelian anyons and is protected from noise and decoherence by the topological properties of these systems. The quantum gates are realized by braiding of these anyons. We propose here an implementation of the  $n$ -qubit topological quantum register in terms of  $2n + 2$  Fibonacci anyons. The matrices emerging from the anyon exchanges, i.e. the *generators* of the braid group for one qubit are derived from the coordinate wave functions of a large number of electron holes and 4 Fibonacci anyons which can furthermore be represented as correlation functions in  $\mathbb{Z}_3$  parafermionic two-dimensional conformal field theory. The representations of the braid groups for more than 4 anyons are obtained by fusing pairs of anyons before braiding, thus reducing eventually the system to 4 anyons.

*Key words:* Topological quantum computation, Conformal field theory, Non-Abelian statistics

*PACS:* 11.25.Hf, 71.10.Pm, 73.40.Hm

---

## 1 Introduction

Quantum technologies have recently experienced a second quantum revolution [1,2]. Quantum computers [3] in particular are expected soon to become more powerful

---

*Email address:* lgeorg@inrne.bas.bg (Lachezar S. Georgiev,).

compared to classical supercomputers and quantum supremacy has been clearly demonstrated in the last 5 years [4,5]. Yet, stable and resilient realizations of qubits and exact execution of the quantum gates are still challenging and insufficient for solving practical physical or mathematical problems.

Topological Quantum Computation (TQC) is an attractive paradigm [6,7,8,9] for quantum computing which uses degenerate multiplets of quantum states to implement the multi-qubit registers. Quantum information is encoded in the fusion channels of non-Abelian anyons [10] and fusion paths Bratteli diagrams [8]. Quantum gates are then executed by braiding (i.e., exchanging clockwise and anti-clockwise) these non-Abelian anyons. Both the information encoding and the quantum gates execution are topologically protected from noise which makes TQC very promising.

The most studied TQC scheme is that of the Ising anyons realized as quasiholes in the Moore–Read Pfaffian Fractional Quantum Hall (FQH) state [11] believed to be observed [12] at filling factor  $\nu = 5/2$ . This FQH state is the most stable one among all states that are expected to possess non-Abelian quasiparticle excitations [12]. However, the Pfaffian FQH state is not capable of universal TQC, since the representation of the Braid group contains only Clifford gates which form a finite subgroup of  $SU(2^n)$  for  $n$  qubits [8,13].

Another FQH state observed experimentally at filling factor  $\nu = 12/5$  in the second Landau level [14], has also attracted much attention. Analytical and numerical arguments suggest that this state might be described by the  $k = 3$  Read–Rezayi state [15] and is believed to possess non-Abelian quasiparticles, which are topologically equivalent to the Fibonacci anyons [7]. The braiding matrices of the Fibonacci anyons, which can be realized in a diagonal CFT coset [16], are non-diagonal and are expected to be universal for topologically protected quantum information processing [17]. However, the energy gap of this FQH state is an order of magnitude lower [14] than that of the FQH state observed at filling factor  $\nu = 5/2$ . This increases drastically the noise/signal ratio at  $\nu = 12/5$ , respectively the stability decreases. Nevertheless, the braiding properties of the Fibonacci anyons, realized by triples of fundamental quasiholes of the  $k = 3$  Read–Rezayi state, have been extensively investigated obtaining remarkable results [18,19,20].

In this paper we propose another implementation of the Fibonacci TQC by using the  $\varepsilon$  primary field of the  $k = 3$  parafermion FQH state realized as a diagonal CFT coset [16]. This scheme is similar to the TQC scheme of Das Sarma et al. [21], which was originally based on monodromy transformations of the Pfaffian wave functions for the Ising Conformal Field Theory (CFT) model. This is done in such a way to construct by braiding the single-qubit Hadamard and phase gates as well as the two-qubit Controlled-Z and Controlled-NOT gates [22,23]. These gate constructions are naturally topologically protected from noise and decoherence.

Compared to the existing TQC models the proposed new topological quantum computation scheme with Fibonacci anyons realized by the  $\varepsilon$  field in the  $\mathbb{Z}_3$  parafermion FQH state is:

- **Natural:** TQC assumes that the different basis vectors in the single-qubit space are realized by the different fusion channels of pairs of anyons. Since there are only 2 fusion channels for the Fibonacci anyons, one qubit is essentially one pair of anyons, just like in the Moore–Read FQH state where the Ising anyons also have 2 fusion channels.
- **Simpler:** The qubit initialization scheme proposed in this paper is similar to but actually simpler than the Ising anyons TQC scheme of [21]. As we will see in Sect. 3 the diagonal coset approach to the Fibonacci TQC described in Ref. [16] is more appropriate than the approach using the  $\widehat{su(3)}_2/u(1)$  because the former naturally inherits the  $\mathbb{Z}_3$  parafermion pairing rule given in Eq. (7) from its Abelian parent as shown in Ref. [16]. *It is this rule that allows us to initialize the Fibonacci TQC using the  $\varepsilon$  fields localized on antidots threaded by one quantum of magnetic flux.*
- **Most economic:** Only  $2n + 2$  Fibonacci anyons are needed to construct an  $n$ -qubit register. Just like in the Ising TQC scheme one pair of anyons is inert (or, as in our case, the first and the last anyons are inert) and serve to compensate the total topological charge of the  $n$ -qubit register. This way the CFT correlation function is non-zero. It is obvious that  $2n + 2$  is the smallest number of Fibonacci anyons needed to construct  $n$  qubits. The Preskill TQC scheme requires  $4n$  Fibonacci anyons for  $n$  qubits [7]. Other schemes using fundamental quasiholes require  $3n$  quasiholes to represent  $n$  qubits [18,19].
- **Most efficient:** The braid matrices in this approach have the smallest dimension compared to the other Fibonacci anyons models. For example, the braid matrices for two qubits, which are realized by 6 Fibonacci anyons have dimension 5 and those for 3 qubits, realized by 8 anyons have dimension 13. Most of the braid generators have a direct sum structure, in an appropriate basis, which makes their explicit derivation almost obvious [24]. This allows us to write the generators of the braid group  $\mathcal{B}^{(n)}$  for Fibonacci anyons for general  $n$  which are given in [24].
- **Universal:** The quantum gates realized by braiding of Fibonacci anyons are known to be capable of universal topological quantum computation in the sense that any quantum gate can be approximated with arbitrary precision by consecutive braids.

*Summary of results:* In Sect. 2 we present general information about the Fibonacci anyons, their Bratteli diagrams and the possibilities to construct qubits. A short introduction to the CFT realization of the  $\mathbb{Z}_3$  parafermion (Read–Rezayi) FQH state is given in Sect. 3. Sect. 4 discusses how to use the CFT four–quasihole wave

functions to construct the elementary qubit's wave-function using the occupation number representation and CFT primary operators. Following the wave-function construction [16] as symmetrization of Abelian CFT correlation functions and the explicit computation in terms of hypergeometric functions [25] we summarize the computation, explicitly given in [24], of the 4-Fibonacci anyons wave function with  $N = 3r$  electron fields where  $r$  is a positive integer. In Sect. 5 we describe the physical realization of the Fibonacci anyons in the  $\mathbb{Z}_3$  parafermion FQH state by the Laughlin argument to localize  $\varepsilon$  fields on antidots threaded by one flux quantum as well as their interferometric measurements. Sect. 6 summarizes the generators of the braid group  $\mathcal{B}^{(4)}$  for 4 Fibonacci anyons and one qubit derived in [24] and we construct explicitly several approximations to the most widely used single-qubit gates. In Sect. 7 we describe the computational basis for two qubits realized by Bratteli diagrams for 6 Fibonacci anyons and summarize the computation, explicitly given in [24], of the generators of the braid group  $\mathcal{B}^{(6)}$ . Then, we show how they can be used to construct various two-qubit gates. In Sect. 8 we describe the computational basis for three qubits realized by Bratteli diagrams for 8 Fibonacci anyon (separating the 8 computational-basis states from the 5 non-computational states) and summarize the computation of the generators of the braid group  $\mathcal{B}^{(8)}$ . How these can be used to construct various three-qubit gates is also shown.

## 2 The Fibonacci anyons and universal TQC: an overview

The  $\mathbb{Z}_3$  parafermion FQH state is one of the few physical systems in which the Fibonacci anyons are believed to be experimentally realizable.

The Fibonacci anyon can be identified with the  $\mathbb{Z}_3$  parafermion primary field of CFT dimension  $2/5$ , denoted by  $\varepsilon$  in Tab. 1

$$\varepsilon \equiv \Phi(\underline{\Lambda}_1 + \underline{\Lambda}_2), \quad \varepsilon^* = \varepsilon, \quad \Delta_\varepsilon = \frac{2}{5},$$

which is self-dual with respect to the  $\mathbb{Z}_3$  parafermion charge conjugation, i.e., it coincides with its antiparticle and can therefore annihilate with itself fusing to the vacuum  $\mathbb{I}$ .

The fusion rules in which will be interested for TQC are those for the two fields  $\mathbb{I}$  and  $\varepsilon$  given in Tab. 2

$$\mathbb{I} \times \mathbb{I} = \mathbb{I}, \quad \mathbb{I} \times \varepsilon = \varepsilon, \quad \varepsilon \times \varepsilon = \mathbb{I} + \varepsilon. \quad (1)$$

The quantum dimension of the Fibonacci anyon  $\varepsilon$  is the Golden ratio  $d_\varepsilon = \delta = \frac{1+\sqrt{5}}{2}$  which follows from the last fusion rule since  $d_\varepsilon^2 = d_\varepsilon + 1$ , or, alternatively,

from the definition of the quantum dimension in terms of modular  $S$  matrix [26,27], i.e.,  $d_\varepsilon = S_{0\varepsilon}/S_{00}$ , with 0 labeling the vacuum sector for the  $\mathbb{Z}_3$  rational CFT.

The multiparticle quantum states of Fibonacci anyons are labeled by fusion paths which are conveniently depicted on the Bratteli diagram shown in Fig. 1. If we start

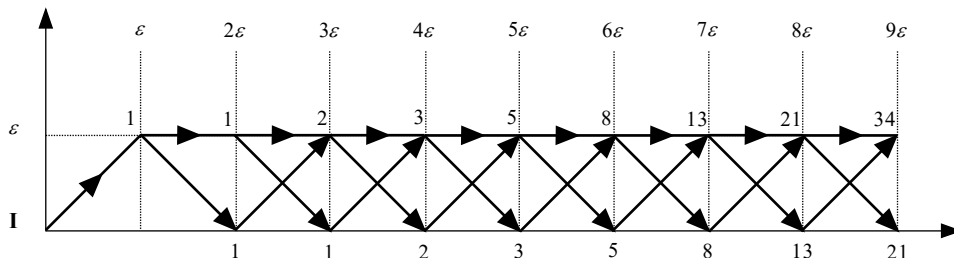


Fig. 1. Bratteli diagram for Fibonacci anyons. Each step to the right adds by fusion one Fibonacci anyon  $\varepsilon$ . On the horizontal axis we mark the vacuum  $\mathbb{I}$  (denoted by  $\mathbf{I}$  in the figure), as the result of the fusion step according to Eq. (1), while on the horizontal dashed line labeled by  $\varepsilon$  we mark the Fibonacci anyon as the result of the fusion step. The numbers next to the vertical dashed lines are the Fibonacci numbers (see the text below).

from the vacuum  $\mathbb{I}$ , which is depicted in Fig. 1 by 1 and add one Fibonacci anyon the result is a single Fibonacci anyon  $\varepsilon$ . This fusion step is denoted by the first arrow in the diagram, which is at  $45^\circ$ . Fusing a second  $\varepsilon$  produces two channels: the vacuum channel, for which the arrow points to  $-45^\circ$  and the  $\varepsilon$  channel, for which the arrow is horizontal pointing to the right. Adding a third  $\varepsilon$  starting from lower channel representing the vacuum on the horizontal axis produces one arrow at  $45^\circ$ , while starting from the  $\varepsilon$  channel of the fusion of the two previous  $\varepsilon$  produces two more arrows to the right: one pointing at  $-45^\circ$  and one horizontal arrow. The numbers written close to the vertical dashed lines representing the number  $n\varepsilon$  of Fibonacci anyons give the number of orthogonal fusion-path states with definite topological charge, i.e., the numbers close to the horizontal axis correspond to the number of orthogonal states with  $n$  of Fibonacci anyons and total topological charge 1 (the vacuum), while the numbers close to the horizontal dashed line denoted by  $\varepsilon$  correspond to the number of orthogonal states with  $n$  of Fibonacci anyons and total topological charge  $\varepsilon$ . It is interesting to note that the multi-anyon state of  $n + 1$  of Fibonacci anyons with trivial topological charge  $\mathbb{I}$  can be obtained in only one way—by adding one  $\varepsilon$  to the multi-anyon state of  $n$  of Fibonacci anyons with total topological charge  $\varepsilon$ . That is why the numbers of states on the two ends of the  $-45^\circ$  arrows are always the same. On the other hand, the multi-anyon state of  $n + 1$  of Fibonacci anyons with total topological charge  $\varepsilon$  can be obtained in two ways—one, by adding one  $\varepsilon$  to the multi-anyon state of  $n$  of Fibonacci anyons with total topological charge  $\varepsilon$  and second, by adding one  $\varepsilon$  to the multi-anyon state of  $n$  of Fibonacci anyons with total topological charge  $\mathbb{I}$ . Therefore, the dimension  $D_{n+1}^{(\varepsilon)}$  of the orthogonal fusion-path states with  $n + 1$  of Fibonacci anyons with total

topological charge  $\varepsilon$  is

$$D_{n+1}^{(\varepsilon)} = D_n^{(\varepsilon)} + D_{n-1}^{(\varepsilon)}, \quad D_1^{(\varepsilon)} = D_2^{(\varepsilon)} = 1, \quad (2)$$

while the dimension  $D_{n+1}^{(\mathbb{I})}$  of the orthogonal fusion-path states with  $n + 1$  of Fibonacci anyons with total topological charge  $\mathbb{I}$  is  $D_{n+1}^{(\mathbb{I})} = D_n^{(\varepsilon)}$ , i.e.,

$$D_{n+1}^{(\mathbb{I})} = D_n^{(\mathbb{I})} + D_{n-1}^{(\mathbb{I})}, \quad D_2^{(\mathbb{I})} = D_3^{(\mathbb{I})} = 1. \quad (3)$$

Because Eqs. (2) and (3) are the recursion relations for the Fibonacci numbers, these dimensions explain the origin of the name of the Fibonacci anyons.

There is an explicit formula for the Fibonacci numbers (2), which can be easily proved by mathematical induction,

$$D_n^{(\varepsilon)} =: D_n = \frac{1}{\sqrt{5}} \left[ \left( \frac{1 + \sqrt{5}}{2} \right)^n - \left( \frac{1 - \sqrt{5}}{2} \right)^n \right]$$

which gives a more physical meaning of the word ‘‘quantum’’ dimension. For large  $n$  the Fibonacci numbers can be approximated by

$$D_n \underset{n \gg 1}{\simeq} \frac{1}{\sqrt{5}} \left( \frac{1 + \sqrt{5}}{2} \right)^n = \text{const} \times (d_\varepsilon)^n$$

because the second term is subleading. Then the physical interpretation is that the dimensions of the Hilbert space spanned by the multianyon wave function corresponding to  $n$  Fibonacci anyons at fixed positions is simply proportional to the quantum dimension  $d_\varepsilon = \delta$  to the power  $n$  [7].

In order to construct a qubit with Fibonacci anyons we need to identify a two-dimensional space of orthogonal fusion-path states and the quantum information encoding is again in the fusion channels and fusion paths. Looking in Fig. 1 we see that there are two different ways to construct a two-dimensional space:  $D_3^{(\varepsilon)} = 2$  or  $D_4^{(\mathbb{I})} = 2$ , i.e., 3 Fibonacci anyons with total topological charge  $\varepsilon$ , as shown in Fig. 2, or 4 Fibonacci anyons with trivial total topological charge  $\mathbb{I}$  as shown in Fig. 4. We have to emphasize here that there is one more fusion-path state, that can be realized with 3 Fibonacci anyons, which has a trivial total topological charge  $\mathbb{I}$  (denoted by  $\mathbf{I}$  in the figure) [7,18,8], as shown in Fig. 3 and is called a non-computational state  $|NC\rangle$ . This state actually decouples from the two states with total topological charge  $\varepsilon$  because  $|NC\rangle$  belongs to a different superselection sector. For this reason all braiding matrices decouple as direct sums for the states  $\{|0\rangle, |1\rangle\}$  and  $|NC\rangle$  as we shall see later. We can write symbolically the fusion channel between two Fibonacci anyons as a subscript of the pair  $(\varepsilon, \varepsilon)_{\mathbb{I}}$  and

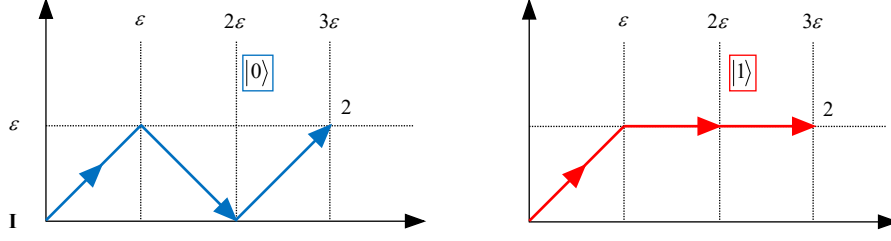


Fig. 2. Bratteli diagrams for the two states in the computational basis  $\{|0\rangle, |1\rangle\}$  of 3 Fibonacci anyons with total topological charge  $\varepsilon$ .

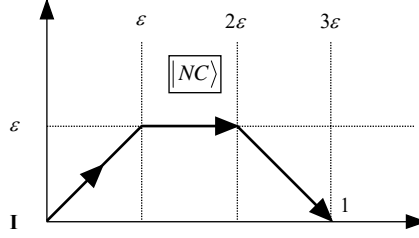


Fig. 3. Bratteli diagram for the non-computational state  $|NC\rangle$  with 3 Fibonacci anyons and trivial total topological charge  $\mathbb{I}$  (denoted by  $\mathbb{I}$  in the figure).

$(\varepsilon, \varepsilon)_\varepsilon$ . Then the fusion path for 3 Fibonacci anyons can be written as  $((\varepsilon, \varepsilon)_\varepsilon, \varepsilon)_\mathbb{I}$  and  $((\varepsilon, \varepsilon)_\varepsilon, \varepsilon)_\varepsilon$ . Now the two computational states and the non-computational state can be written as [18]

$$\begin{aligned} |0\rangle &= ((\varepsilon, \varepsilon)_\mathbb{I}, \varepsilon)_\varepsilon \\ |1\rangle &= ((\varepsilon, \varepsilon)_\varepsilon, \varepsilon)_\varepsilon \\ |NC\rangle &= ((\varepsilon, \varepsilon)_\varepsilon, \varepsilon)_\mathbb{I}. \end{aligned}$$

Another way to represent a qubit, which is more appropriate for the CFT implementation, is to use 4 Fibonacci anyons with total topological charge  $\mathbb{I}$ . The dimension of the Hilbert space is 2 as can be seen from Fig. 1. In that case the computational basis  $\{|0\rangle, |1\rangle\}$  of the fusion-path states is shown in Fig. 4 and can be written symbolically as CFT correlation functions with fixed fusion channels and fusion paths corresponding to the Bratteli diagrams shown in Fig. 4

$$\begin{aligned} |0\rangle &= \langle(((\varepsilon, \varepsilon)_\mathbb{I}, \varepsilon)_\varepsilon, \varepsilon)_\mathbb{I}\rangle = \langle(\varepsilon, \varepsilon)_\mathbb{I}, (\varepsilon, \varepsilon)_\mathbb{I}\rangle \\ |1\rangle &= \langle(((\varepsilon, \varepsilon)_\varepsilon, \varepsilon)_\varepsilon, \varepsilon)_\mathbb{I}\rangle = \langle(\varepsilon, \varepsilon)_\varepsilon, (\varepsilon, \varepsilon)_\varepsilon\rangle, \end{aligned} \quad (4)$$

where we used the associativity of the fusion rules which allows to fuse the first and the last pair of anyons and then to fuse further the resulting anyons. For example, in the state  $|1\rangle$  the first two Fibonacci anyons fuse through the channel  $\varepsilon \times \varepsilon \rightarrow \varepsilon$  and so do the last two Fibonacci anyons. After the fusion of the first and the last

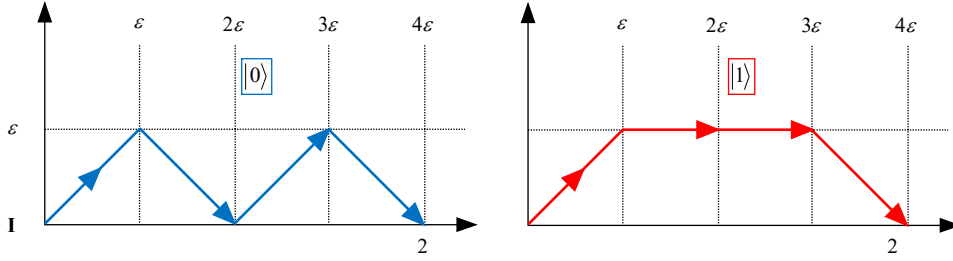


Fig. 4. Bratteli diagrams for the computational basis  $\{|0\rangle, |1\rangle\}$  of 4 Fibonacci anyons with total topological charge  $\mathbb{I}$  (denoted by  $\mathbf{I}$  in the figure).

pairs of anyons the resulting two  $\varepsilon$  inside the CFT correlation function in the state  $|1\rangle$  in Eq. (4) fuse further to  $\mathbb{I}$  because the second channel gives zero contribution due to  $\langle\varepsilon\rangle = 0$  which holds in the CFT. One advantage of this representation of a qubit is that there is no non-computational state and therefore no leakage out of the single-qubit's Hilbert space. We will consider in more detail the CFT realization of the single qubit in Sect. 4 below. This pair representation of the qubits is similar to that in the Ising model where quantum information is encoded in the fusion channel of the first pair of Ising anyons, while the last pair of anyons is inert (or, vice versa). This means that it carries no information and only ensures that the CFT correlation function is not zero [23].

### 3 The $\mathbb{Z}_3$ parafermion fractional quantum Hall state

The  $\mathbb{Z}_3$  parafermion (Read–Rezayi) state is the most promising candidate to describe the experimentally observed [28,29,30] incompressible state in the second Landau level, corresponding to filling factor  $\nu_H = 12/5 = 3 - 3/5$ . The most appealing characteristics of this FQH state is that it possesses non-Abelian quasiparticle excitations, which are topologically equivalent to the Fibonacci anyons [18,8]. These anyons can be used to construct multielectron wave functions which belong to degenerate manifolds (of wave functions with electrons and anyons at fixed positions) whose dimension increases exponentially with the number of anyons and can be used for *universal* topologically protected quantum information processing [18,8]. While the  $\nu_H = 12/5$  FQH state is less stable than the more popular  $\nu_H = 5/2$  FQH state, which is believed to be described by the Majorana fermion of the Ising model, the latter is known to be not universal [13], in the sense that not all elementary quantum operations can be implemented by braiding Ising anyons [23,8] and are therefore not topologically protected. On the contrary, all elementary quantum gates in the Fibonacci quantum computer can be implemented by braiding of Fibonacci anyons [18] and all they are fully protected from noise and decoherence by the topology of the quantum computer [8].



The rational CFT describing the  $\mathbb{Z}_3$  parafermion FQH state has been constructed [16] as a diagonal coset of a parent Abelian CFT, whose charges form a maximally symmetric chiral quantum Hall lattice in the terminology of [31] and can be represented as a direct sum

$$\left(\widehat{u(1)}_{15} \oplus \text{PF}_3\right)^{\mathbb{Z}_3}, \quad \text{PF}_3 = \frac{\widehat{su(3)}_1 \oplus \widehat{su(3)}_1}{\widehat{su(3)}_2}. \quad (5)$$

Here  $\widehat{u(1)}_{15}$  is the  $u(1)$  current algebra, rationally extended with a pair of vertex exponents  $:\exp(\pm i\sqrt{15}\phi(z)):$  of a normalized chiral boson  $\phi(z)$ , i.e.,

$$\langle\phi(z)\phi(w)\rangle = -\ln(z-w). \quad (6)$$

This  $u(1)$  algebra represents the electric properties of the edge excitations in the FQH liquid. The neutral part  $\text{PF}_3$  is a diagonal coset construction with Virasoro central charge  $4/5$  [16] of the current algebra  $\widehat{su(3)}_1 \oplus \widehat{su(3)}_1$  factorized by its diagonal subalgebra  $\widehat{su(3)}_2$  generated by the sums of the generators of the numerator in  $\text{PF}_3$ . The neutral sector has no contribution to the electric properties but describes other topological properties of the edge excitations, such as the statistical angle, fusion and braiding of particle-like excitations. The  $\mathbb{Z}_3$  superscript in Eq. (5)

$\underline{\Lambda}_\mu + \underline{\Lambda}_\nu$	$\Delta(\underline{\Lambda}_\mu + \underline{\Lambda}_\nu)$	$P$	$\sigma$	$Q$	$\mathbb{Z}_3$ Field
$\underline{\Lambda}_0 + \underline{\Lambda}_0$	0	0	0	0	$\mathbb{I}$
$\underline{\Lambda}_0 + \underline{\Lambda}_1$	$\frac{1}{15}$	1	1	1	$\sigma_1$
$\underline{\Lambda}_0 + \underline{\Lambda}_2$	$\frac{1}{15}$	2	2	2	$\sigma_2$
$\underline{\Lambda}_1 + \underline{\Lambda}_1$	$\frac{2}{3}$	2	0	1	$\psi_1$
$\underline{\Lambda}_1 + \underline{\Lambda}_2$	$\frac{2}{5}$	0	1	2	$\varepsilon$
$\underline{\Lambda}_2 + \underline{\Lambda}_2$	$\frac{2}{3}$	1	0	2	$\psi_2$

Table 1

Quantum numbers for the diagonal coset (5): the weight of the coset primary field, its conformal dimension  $\Delta$ ,  $\mathbb{Z}_3$  charge  $P = \mu + \nu \bmod 3$ ,  $\sigma$ ,  $Q$  and field notation.

represents the  $\mathbb{Z}_3$ -pairing rule for combining charged and neutral excitations. This is a general pairing rule which applies for all FQH states' CFTs for which the numerator of the filling factor is  $n_H > 1$  [32]. In our case the  $\mathbb{Z}_3$  pairing rule is simply

$$\mu + \nu = l \bmod 3 \quad (7)$$

where  $\underline{\Lambda}_\mu + \underline{\Lambda}_\nu$  labels the parafermion primary field given in Table 1 and  $l \bmod 3$  labels the  $\widehat{u(1)}$  primary field  $:\exp(i\frac{l}{\sqrt{15}}\phi(z)):$ .

The full chiral partition functions of the  $\mathbb{Z}_3$  parafermion FQH state is given by [16]

$$\chi_{l,\rho}(\tau, \zeta) = \sum_{s=0}^2 K_{l+5s}(\tau, 3\zeta; 15) \text{ch}(\underline{\Lambda}_{l-\rho+s} + \underline{\Lambda}_{\rho+s})(\tau) \quad (8)$$

and describes the spectrum of the edge excitations of the different topological sectors of the CFT (5). Here the charge label is defined  $l \bmod 5$  and the neutral label is defined  $\rho \bmod 3$  with the natural restriction  $l - \rho \leq \rho$  [16,33]. The characters of the irreducible representations of the diagonal coset (5) labeled by the weight  $\underline{\Lambda}_\mu + \underline{\Lambda}_\nu$  are denoted as  $\text{ch}(\underline{\Lambda}_\mu + \underline{\Lambda}_\nu)(\tau)$  and  $K_l(\tau, \zeta; m)$  are the  $\widehat{u(1)}$  partition functions for the charged part which is completely determined by the filling factor  $\nu_H$  and coincides with that for a chiral Luttinger liquid with a compactification radius [34]  $R_c = 1/m$ , in the notation of [26,35]

$$K_l(\tau, \zeta; m) = \frac{\text{CZ}}{\eta(\tau)} \sum_{n=-\infty}^{\infty} q^{\frac{m}{2}(n+\frac{l}{m})^2} e^{2\pi i \zeta(n+\frac{l}{m})}. \quad (9)$$

Here  $q = e^{2\pi i \tau} = e^{-\beta \Delta \varepsilon}$ , where  $\beta = (k_B T)^{-1}$  is the inverse temperature,  $\Delta \varepsilon = \hbar v_c / L$  is the non-interacting energy spacing on the edge,

$$\eta(\tau) = q^{1/24} \prod_{n=1}^{\infty} (1 - q^n)$$

is the Dedekind function [26] and  $\text{CZ}(\tau, \zeta) = \exp(-\pi \nu_H (\text{Im } \zeta)^2 / \text{Im } \tau)$  is the Cappelli–Zemba factor needed to preserve the invariance of  $K_l(\tau, \zeta; m)$  with respect to the Laughlin spectral flow [34].

The modular parameter  $\zeta$  used in the definition of the rational CFT partition functions is related to the chemical potential  $\mu_c$  by [35,36]

$$\zeta = \frac{\mu_c}{\Delta \varepsilon} \tau, \quad \text{where} \quad \tau = i\pi \frac{T_0}{T}, \quad T_0 = \frac{\hbar v_c}{\pi k_B L} \quad (10)$$

and transforms after introducing Aharonov–Bohm flux  $\phi$  as [16,36]

$$\zeta \rightarrow \zeta + \phi \tau \quad \iff \quad \mu_c \rightarrow \mu_c + \phi \Delta \varepsilon. \quad (11)$$

The neutral partition functions  $\text{ch}(\underline{\Lambda}_\mu + \underline{\Lambda}_\nu)(\tau)$  of the diagonal coset  $\text{PF}_3$  are labeled in principle by an admissible weight for the current algebra  $\widehat{su(3)}_2$ , which can be written as a sum of two fundamental  $su(3)$  weights, i.e.,  $\underline{\Lambda}_\mu + \underline{\Lambda}_\nu$  with  $0 \leq \mu \leq \nu \leq 2$ . Following [16] (and the references therein) these characters for the diagonal

coset CFT can be written as

$$\text{ch}_{\sigma,Q}(\tau; \text{PF}_3) = q^{\Delta^{\text{PF}}(\sigma) - \frac{1}{30}} \sum_{\substack{m_1, m_2=0 \\ m_1+2m_2 \equiv Q \pmod{3}}}^{\infty} \frac{q^{\underline{m} \cdot C^{-1} \cdot (\underline{m} - \underline{\Lambda}_\sigma)}}{(q)_{m_1} (q)_{m_2}}, \quad (12)$$

where  $(q)_n = \prod_{j=1}^n (1 - q^j)$ ,  $\underline{m} = (m_1, m_2)$  is a 2 component vector with non-negative integer components in the basis of  $su(3)$  fundamental weights  $\{\underline{\Lambda}_1, \underline{\Lambda}_2\}$ ,  $\Delta^{\text{PF}}(\underline{\Lambda}_\sigma) = \sigma(3 - \sigma)/30$  is the CFT dimension of the primary field characterized by the coset triple [16] of weights  $(\underline{\Lambda}_\sigma, 0; \underline{\Lambda}_0 + \underline{\Lambda}_\sigma)$ , for  $\underline{\Lambda}_\sigma \in \{0, \underline{\Lambda}_1, \underline{\Lambda}_2\}$  and  $C^{-1}$  is the inverse  $su(3)$  Cartan matrix [26,35].

The parafermion characters  $\text{ch}_{\sigma,Q} \equiv \text{ch}(\underline{\Lambda}_\mu + \underline{\Lambda}_\nu)$  derived in Eq. (12) are the true characters [16] of the diagonal coset  $\text{PF}_3$  labeled in the standard way by the level-2 weights  $\underline{\Lambda}_\mu + \underline{\Lambda}_\nu$ , where  $0 \leq \mu \leq \nu \leq 2$ . Then the parameters  $(\sigma, Q)$  are related to  $(\mu, \nu)$  by [16]

$$\sigma = \nu - \mu, \quad Q = \nu \quad \iff \quad \mu = Q - \sigma, \quad \nu = Q. \quad (13)$$

The partition functions given in Eqs. (8), (9) and (12) will be used in Sect. 5.1 to identify the quasiparticles which will be localized on the antidot's edge in response to threading the antidot with one quantum of Aharonov–Bohm flux and this will be the initialization procedure for the Fibonacci TQC. The fusion rules for the  $\mathbb{Z}_3$  parafermion fields are given in Tab. 2.

$\sigma_1 \times \sigma_1 = \sigma_2 \oplus \psi_1$	$\sigma_2 \times \sigma_2 = \sigma_1 \oplus \psi_2$	$\psi_1 \times \psi_1 = \psi_2$
$\sigma_1 \times \sigma_2 = \mathbb{I} \oplus \varepsilon$	$\sigma_2 \times \psi_1 = \sigma_1$	$\psi_1 \times \varepsilon = \sigma_2$
$\sigma_1 \times \psi_1 = \varepsilon$	$\sigma_2 \times \varepsilon = \sigma_2 \oplus \psi_1$	$\psi_1 \times \psi_2 = 1$
$\sigma_1 \times \varepsilon = \sigma_1 \oplus \psi_2$	$\sigma_2 \times \psi_2 = \varepsilon$	$\varepsilon \times \varepsilon = \mathbb{I} \oplus \varepsilon$
$\sigma_1 \times \psi_2 = \sigma_2$	$\psi_2 \times \psi_2 = \psi_1$	$\varepsilon \times \psi_2 = \sigma_1$

Table 2

Fusion rules for the primary fields defined in Table 1 within the diagonal-coset realization of the  $\mathbb{Z}_3$  parafermions.

#### 4 Four-quasihole wave functions and the elementary qubit

The universality classes of the FQH states, including their topological properties, can be well described by the effective CFT for the edge excitations in the thermodynamic limit [31,34,11]. Since we intend to obtain the elementary braid matrices

by explicitly exchanging the coordinates of the Fibonacci anyons we need to find the coordinate wave functions for a number of anyons and a (big) number  $N$  of electrons representing the incompressible FQH liquid. To this end we need to realize the quantum states with many Fibonacci anyons as correlation functions of the  $\mathbb{Z}_3$  parafermion CFT.

We start with the ground state of the  $\mathbb{Z}_3$  parafermion FQH state, i.e, the state with  $N$  electrons but without quasiparticle excitations, which can be written as [15,16]

$$\Phi_{\text{GS}}(z_1, \dots, z_N) = \langle Q_{\text{bg}} | \prod_{i=1}^N \psi_{\text{hole}}(z_i) | 0 \rangle \exp \left( -\frac{1}{4} \sum_{j=1}^N |z_j|^2 \right)$$

where the exponent represents the standard Gaussian factor for the Landau problem (we set the magnetic length  $l = \sqrt{2/eB} = 1$ ) and the first factor is the correlation function of the electron hole field operators computed in the  $\mathbb{Z}_3$  parafermion CFT.  $N$  is the number of electrons with coordinates  $z_i$  and must be equal to  $3r$  with  $r$  an integer because the electron fields have a non-trivial  $\mathbb{Z}_3$  parafermion charge and must be created in triples [15,16]. Here  $\psi_{\text{hole}}(z_i)$  is the electron hole operator [16] representing an electron hole with coordinate  $z$

$$\psi_{\text{hole}}(z) = : \exp \left( i \sqrt{\frac{5}{3}} \phi(z) \right) : \psi_1(z), \quad \psi_1(z) \equiv \Phi(\underline{\Lambda}_1 + \underline{\Lambda}_1)(z) \quad (14)$$

of a  $\widehat{u(1)}$  vertex exponent of a normalized chiral boson field with charge  $1/\sqrt{\nu_H}$  and the  $\mathbb{Z}_3$  parafermion primary field  $\psi_1(z) \equiv \Phi(\underline{\Lambda}_1 + \underline{\Lambda}_1)(z)$  whose CFT dimension is  $2/3$  in the notation of [16]. The electric charge of the electron field is 1 (in units in which  $e = h = 1$ ) and because of the charge-flux relation (29) it carries fractional magnetic flux - the quantization of the magnetic flux in FQH liquids is the physical reason why the electrons in the ground state must be created in triples. The total conformal dimension of the electron is

$$\Delta_{\text{hole}} = \frac{1}{2} \left( \sqrt{\frac{5}{3}} \right)^2 + \frac{2}{3} = \frac{3}{2}$$

as it should be for a fermion field. It is worth emphasizing that the CFT dimension of the  $\widehat{u(1)}$  part of the electron operator is fixed by the filling factor  $\nu_H = 3/5$  to be  $(1/2)(5/3)$  and twice this number is the statistical angle of the electron field. It is obvious that there should be a non-trivial neutral component of the electron field operator so that the total CFT dimension would be half-odd integer. This neutral part of the electron field here is given by the parafermion current  $\psi_1(z)$ .

The state denoted by  $\langle Q_{\text{bg}} |$  is the CFT conjugate [26] of the CFT state in the occupation number representation which can be obtained by fusing all charged and

fields to the center  $z_0 = 0$  of the FQH disk

$$|Q_{\text{bg}}\rangle = \lim_{z_0 \rightarrow 0} : \exp(iQ_{\text{bg}}\phi(z_0)) : |0\rangle$$

where  $Q_{\text{bg}} = N\sqrt{\frac{5}{3}}$  is the  $u(1)$  charge of the state with all electric charges concentrated at the origin of the disk. Using the CFT rule for state conjugation [26] we have

$$\langle Q_{\text{bg}}| = \lim_{z_0 \rightarrow \infty} z_0^{2\Delta_l} \langle 0| : \exp(-iQ_{\text{bg}}\phi(z_0)) :$$

with  $\Delta_l = (Q_{\text{bg}})^2/2 = 5N^2/6$ .

Traditionally in the literature on QH states the quantity  $Q_{\text{bg}}$  has been called the background charge or screening charge which is plugged into the CFT correlation function in order to make it non-zero. However  $Q_{\text{bg}}$  in our case plays a more fundamental role because it can be interpreted as the representation of the state of the FQH system in the occupation number representation. Because we are interested in the braid behavior of the anyons we need a coordinate many-body wave function  $\Phi(x_1, \dots, x_N)$  which can be obtained from the quantum state  $|\Phi_N\rangle = |Q_{\text{bg}}\rangle$  in the occupation number representation using the standard relation (cf. Eq. (117) in Ref. [37])

$$\begin{aligned} |\Phi_N\rangle &= \frac{1}{\sqrt{N!}} \int d\mathbf{x}_1 \dots d\mathbf{x}_N \Phi(\mathbf{x}_1, \dots, \mathbf{x}_N) \hat{\Psi}^\dagger(\mathbf{x}_N) \dots \hat{\Psi}^\dagger(\mathbf{x}_1) |0\rangle \iff \\ \Phi^*(\mathbf{x}_1, \dots, \mathbf{x}_N) &= \frac{1}{\sqrt{N!}} \langle \Phi_N | \hat{\Psi}^\dagger(\mathbf{x}_N) \dots \hat{\Psi}^\dagger(\mathbf{x}_1) |0\rangle, \end{aligned} \quad (15)$$

where  $\hat{\Psi}(\mathbf{x}) = \sum_n \hat{a}_n \psi_n(\mathbf{x})$  is the electron field operator ( $\hat{a}_n, n = 0, \dots, \infty$  are the fermionic annihilation operators) satisfying together with its Hermitian conjugate  $\hat{\Psi}^\dagger(\mathbf{x})$  the canonical anticommutation relations  $\{\hat{\Psi}(\mathbf{x}), \hat{\Psi}^\dagger(\mathbf{x}')\} = \delta(\mathbf{x} - \mathbf{x}')$  [37].

In a similar way we shall construct the coordinate wavefunction for  $N$  electron holes and 4 Fibonacci anyons, with coordinates  $w_a$  in the plane, which we shall use as qubit (from now on we skip the standard Gaussian exponent and leave only the holomorphic part)

$$\Phi_{4F}(\{w_a\}; \{z_i\}) = \langle Q_{\text{bg}}, \Lambda | \psi_F(w_1) \psi_F(w_2) \psi_F(w_3) \psi_F(w_4) \prod_{i=1}^N \psi_{\text{hole}}(z_i) |0\rangle, \quad (16)$$

where  $\psi_F(w)$  is the field operator representing a Fibonacci anyon with coordinate  $w$  in the complex plane as a primary field in the  $u(1) \times \text{PF}_3$  CFT

$$\psi_F(w) = : e^{i\frac{3}{\sqrt{45}}\phi(w)} : \varepsilon(w) \quad (17)$$

with  $\varepsilon(w)$  being the coset CFT primary field of dimension  $\Delta = 2/5$ , labeled by the weight  $\underline{\Lambda}_1 + \underline{\Lambda}_2$ , with coordinate  $w$  in the complex plane. We point out here that the  $\mathbb{Z}_3$  parafermion charge of the field  $\varepsilon(w)$  is 0 and the magnetic flux corresponding to  $\varepsilon(w)$  is integer. Therefore there is no clustering of the  $\varepsilon(w)$  fields and all correlation functions of arbitrary number of  $\varepsilon(w)$  might be non-zero (again the number of electrons must be  $N = 3r$  with  $r$  integer). It is important to note also that the Fibonacci anyon field (17) must be relatively local with the electron field (14), see assumption (A4) in [31], which is indeed the case as can be seen from the operator product expansion (OPE normalization is the same as in Ref. [25])

$$\psi_{\text{hole}}(z)\psi_F(w) \underset{z \rightarrow w}{\simeq} \frac{2}{\sqrt{3}} : e^{i\frac{8}{\sqrt{15}}\phi(w)} : \sigma_2(w) + O(z-w) \quad (18)$$

The occupation number representation state denoted by  $\langle Q_{\text{bg}}, \Lambda |$  is now the CFT conjugate of the CFT state which is this time obtained by fusing all charged and parafermion fields to the origin  $z_0 = 0$

$$|Q_{\text{bg}}, \Lambda\rangle = \lim_{z_0 \rightarrow 0} : \exp(iQ_{\text{bg}}\phi(z_0)) : \Phi_\Lambda(z_0) |0\rangle$$

where  $Q_{\text{bg}} = 4\frac{3}{\sqrt{15}} + N\sqrt{\frac{5}{3}}$  is the  $\widehat{u(1)}$  charge of the state with all electric charges concentrated at the origin (of the FQH disk) and  $\Phi_\Lambda(z_0)$  is the  $\mathbb{Z}_3$  parafermion field with weight  $\Lambda$  which is the result of the fusion of all parafermion topological charges at the origin. Using the CFT rule for state conjugation [26] we have

$$\langle Q_{\text{bg}}, \Lambda | = \lim_{z_0 \rightarrow \infty} z_0^{2(\Delta_l + \Delta_\Lambda)} \langle 0 | : \exp(-iQ_{\text{bg}}\phi(z_0)) : \Phi_\Lambda^*(z_0)$$

with  $\Delta_l = (Q_{\text{bg}})^2/2 = (12 + 5N)^2/30$  and  $\Delta_\Lambda$  is the CFT dimension of the parafermion field  $\Phi_\Lambda(z_0)$ .

Writing explicitly the correlation function of the  $\widehat{u(1)}$  part, which is of Laughlin type, and separately the correlation function in the  $\mathbb{Z}_3$  parafermion part, we obtain the wave function for 4  $\varepsilon$  fields and  $N = 3r$  electrons with  $r$  integer (we denote by  $\langle \Lambda |$  the CFT conjugate of  $|\Lambda\rangle = \Phi_\Lambda(0)|0\rangle$ )

$$\Psi_{4F}(w_1, \dots, w_4; z_1, \dots, z_N) = \langle \Lambda | \varepsilon(w_1)\varepsilon(w_2)\varepsilon(w_3)\varepsilon(w_4) \prod_{i=1}^N \psi_1(z_i) |0\rangle_{\text{PF}} \times \prod_{1 \leq a < b \leq 4} (w_a - w_b)^{\frac{3}{5}} \prod_{a=1}^4 \prod_{i=1}^N (w_a - z_i) \prod_{1 \leq i < j \leq N} (z_i - z_j)^{\frac{5}{3}} \quad (19)$$

where now the remaining correlation function is only in the (neutral) parafermion CFT and again  $\psi_1(z)$  is given in Eq. (14). Following Ref. [25] and using this decom-

position of the 4 Fibonacci anyon wave function we will obtain the braid matrices for exchanging Fibonacci anyons in Sect. 6.

As can be seen from Fig. 1 the register containing  $n$  Fibonacci anyons  $\varepsilon$  can fuse at the origin of the FQH disk either to  $\mathbb{I}$  or to  $\varepsilon$  so that the weight in Eq. (19) can only be  $\Lambda = \mathbb{I}$ , or  $\Lambda = \varepsilon$ . This is an overall topological characteristics of the quantum register which can be interpreted as a  $\mathbb{Z}_3$  topological charge at infinity. It can be measured in electronic Fabri–Perot interferometers by transporting single non-Abelian quasiparticles ( $\sigma_1$  or  $\sigma_2$ ) around the register, see Sect. 5.2. This topological characteristics cannot be changed during the processes of braiding. Therefore for any number  $n$  of  $\varepsilon$  fields there will be two decoupled representations of the braid group  $\mathcal{B}^{(n)}$  which we shall label by a subscript of the left bra-vector. For  $n = 4$  we have

$$\mathbb{I}\langle\varepsilon(w_1)\varepsilon(w_2)\varepsilon(w_3)\varepsilon(w_4)\rangle, \quad \varepsilon\langle\varepsilon(w_1)\varepsilon(w_2)\varepsilon(w_3)\varepsilon(w_4)\rangle \quad (20)$$

where we have skipped the product  $\prod_{i=1}^N \psi_1(z_i)$  for convenience.

There is one simple but very important observation that correlation function of a single  $\varepsilon$  field and an arbitrary product of parafermion fields  $\psi_1(z_i)$  vanishes

$$\mathbb{I}\left\langle\varepsilon(w)\prod_{i=1}^N\psi_1(z_i)\right\rangle_{\text{PF}} \equiv 0, \quad \varepsilon\left\langle\varepsilon(w)\prod_{i=1}^N\psi_1(z_i)\right\rangle_{\text{PF}} \neq 0$$

while the correlation function of a single  $\varepsilon$  field and an arbitrary product of parafermion fields  $\psi_1(z_i)$  in the  $\varepsilon$ -representation can be non-zero. Because of the  $\Lambda = \varepsilon$  case in Eq. (20) a single  $\varepsilon$  field can indeed be localized on an antidot which is the initialization scenario for the Fibonacci quantum computer, see Sect. 5.1.

From now on we will consider only the representations corresponding to  $\Lambda = \mathbb{I}$ . Using the relative locality of the fundamental  $\mathbb{Z}_3$  quasihole  $\psi_{\text{qh}}(w)$  with the electron field (14), namely

$$\psi_{\text{qh}}(w) = :e^{i\frac{1}{\sqrt{15}}\phi(w)}: \sigma_1(w), \quad \psi_{\text{hole}}(z)\psi_{\text{qh}}(w) \underset{z \rightarrow w}{\simeq} \sqrt{\frac{2}{3}} :e^{i\frac{6}{\sqrt{15}}\phi(w)}: \varepsilon(w) \quad (21)$$

we can express the  $\mathbb{Z}_3$  parafermion CFT blocks  $\Psi_{4\varepsilon}(w_a; z_i)$  corresponding to the basis vectors, labeled by superscript 0 or 1, of the single-qubit space (19) in terms of the  $\mathbb{Z}_3$  parafermion correlation function of 4 fields  $\sigma_1$  and  $3r + 4$  fields  $\psi_1$  as follows

$$\Psi_{4\varepsilon}(w_a; z_i)^{(0,1)} = \langle\varepsilon(w_1)\varepsilon(w_2)\varepsilon(w_3)\varepsilon(w_4)\prod_{i=1}^{3r}\psi_1(z_i)\rangle_{\text{PF}}^{(0,1)} =$$

$$\frac{9}{4} \prod_{1 \leq a < b \leq 4} (w_a - w_b)^{-\frac{1}{3}} \prod_{a=1}^4 \prod_{i=1}^{3r} (w_a - z_i)^{-\frac{5}{3}} \times \lim_{w'_a \rightarrow w_a} \langle \sigma_1(w_1) \sigma_1(w_2) \sigma_1(w_3) \sigma_1(w_4) \prod_{a=1}^4 \psi_1(w'_a) \prod_{i=1}^{3r} \psi_1(z_i) \rangle_{\text{PF}}^{(0,1)}. \quad (22)$$

Following [16], the last correlation function of 4 quasiholes and  $N = 3r + 4$  electrons in Eq. (22) was expanded in Ref. [25] in terms of the functions  $\Psi_{(12)(34)}(w_a, z_a, z_i)$  and  $\Psi_{(13)(24)}(w_a, z_a, z_i)$  reflecting the two independent ways of splitting the 4 anyons into two pairs (like in the Moore–Read FQH state [11]). The coefficient functions (depending on  $w_a, a = 1, \dots, 4$ ) computed in [25] were expressed in terms of hypergeometric functions [38] of certain harmonic ratio.

These results were used in Ref. [24] to present, after taking the limit  $w'_a \rightarrow w_a$ , the correlation function (22) for any integer  $r$  as

$$\langle \varepsilon(w_1) \varepsilon(w_2) \varepsilon(w_3) \varepsilon(w_4) \prod_{i=1}^{3r} \psi_1(z_i) \rangle_{\text{PF}}^{(p)} = \Phi^{(p)}(\{w\}, \{z\}), \quad p = 0, 1 \quad (23)$$

where

$$\begin{aligned} \Phi^{(0)}(\{w\}, \{z\}) &= Q [(w_{12}w_{34})^{-3} \eta^3 (1 - \eta)^{-\frac{3}{2}}] (w_{12}w_{34})^{-\frac{4}{5}} (1 - \eta)^{\frac{1}{10}} \times \\ &\times \left[ F\left(\frac{1}{5}, \frac{4}{5}, \frac{3}{5}; \eta\right) \Psi_{12,34} - \frac{1}{3} F\left(\frac{6}{5}, \frac{4}{5}, \frac{8}{5}; \eta\right) \Psi_{13,24} \right], \quad (24) \\ \Phi^{(1)}(\{w\}, \{z\}) &= C Q [(w_{12}w_{34})^{-3} \eta^3 (1 - \eta)^{-\frac{3}{2}}] (w_{12}w_{34})^{-\frac{4}{5}} \eta^{-\frac{3}{5}} (1 - \eta)^{-\frac{3}{10}} \\ &\times \left[ \eta F\left(\frac{1}{5}, \frac{4}{5}, \frac{7}{5}; \eta\right) \Psi_{12,34} - 2 F\left(\frac{1}{5}, -\frac{1}{5}, \frac{2}{5}; \eta\right) \Psi_{13,24} \right]. \quad (25) \end{aligned}$$

Here  $w_{ab} = w_a - w_b$ ,  $\eta = \frac{w_{12}w_{34}}{w_{13}w_{24}}$ ,  $2C = \sqrt{\frac{\Gamma(1/5)\Gamma^3(3/5)}{\Gamma(4/5)\Gamma^3(2/5)}}$  and

$$Q = Q(\{w\}, \{z\}) := \frac{9}{4} \prod_{a=1}^4 \prod_{i=1}^{3r} (w_a - z_i)^{-1} \prod_{1 \leq j < k \leq 3r} (z_j - z_k)^{-\frac{2}{3}}, \quad (26)$$

with  $\{w\} = \{w_1, \dots, w_4\}$  and  $\{z\} = \{z_1, \dots, z_{3r}\}$ . The factors  $\Psi_{12,34}$  and  $\Psi_{13,24}$  are polynomials in (the differences of)  $\{w\}$  and  $\{z\}$  defined as

$$\begin{aligned} \Psi_{12,34} &= \Psi_{12,34}(\{w\}, \{z\}) := \Psi_{(12)(34)}(w_a, w_a, z_i), \\ \Psi_{13,24} &= \Psi_{13,24}(\{w\}, \{z\}) := \Psi_{(13)(24)}(w_a, w_a, z_i). \end{aligned} \quad (27)$$

The result in Eq. (23) was obtained (for slightly different limits) in Ref. [25] only for  $r = 0$ . However, a wave function representation in terms of CFT correlators like the one in Eq. (16) only has physical meaning describing the FQH state in the



thermodynamic limit  $N = 3r \rightarrow \infty$ . The needed generalization to any positive integer  $r$  (presumably,  $r \gg 1$ ) has been carefully derived in Ref. [24].

The 4-anyon wavefunctions (24) and (25) will be our starting point for the derivation of the generators of the braid group  $\mathcal{B}_4$  for 4 Fibonacci anyons in the  $\mathbb{Z}_3$  parafermion FQH state. To this end, one does not need to know the explicit form of the factors (27). It is sufficient to take into account the Nayak-Wilczek type relation connecting the ones corresponding to the three possible ways of splitting 4 anyons into two pairs which, written in terms of the harmonic ratio  $\eta$  reads

$$\eta \Psi_{12,34} - \Psi_{13,24} + (1 - \eta) \Psi_{14,23} = 0 \quad (28)$$

with  $\Psi_{14,23}$  defined analogously to (27), cf. Refs. [25,24].

## 5 Fibonacci anyons in the $\mathbb{Z}_3$ parafermion FQH state

### 5.1 Initialization of the Fibonacci qubit

The construction of the qubit for Fibonacci anyons is similar to that for the Ising anyons proposed by Das Sarma et al. [21]. Consider a quantum antidot inside of a FQH bar with  $\mathbb{Z}_3$  parafermion liquid with  $\nu_H = 3/5$ , as shown in Fig. 5. The

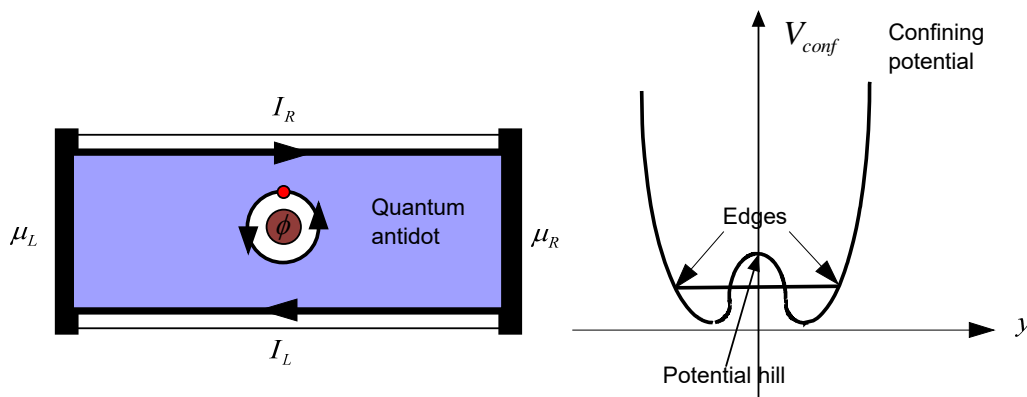


Fig. 5. An antidot is an island (in white) inside of a quantum Hall liquid (in blue) with filling factor  $\nu_H = 3/5$ . The arrows show the direction of the edge currents along the edges and along the perimeter of the antidot. The chemical potentials on the left and right contacts are denoted by  $\mu_L$  and  $\mu_R$ .

antidot is created by adding a potential hill, shown on the right in Fig. 5, to the confining potential  $V_{conf}$  creating the FQH bar. This potential hill creates an island

in the FQH liquid whose edge accommodates edge current due to the magnetic field. Next, we increase adiabatically the magnetic flux threading the antidot until it reaches one quantum of Aharonov–Bohm flux  $\phi = h/e = 1$  where  $h$  is the Plank constant and  $e$  is the charge of the electron (we can think of the flux as created by an infinitely thin solenoid). This is depicted in Fig. 5 by the brown disk inside the antidot with the symbol  $\phi$  inside it. Now the incompressible quantum Hall liquid surrounding the antidot responds to the flux threading the antidot by localizing one or several quasiholes/quasiparticles along the edge of the antidot, depicted by the small red circle on the antidot’s edge, in such a way to compensate the flux  $\phi$ . The electric charge of the quasiparticle localized on the antidot is uniquely determined by the universal quantum Hall flux–charge relation [31,16]

$$Q_{\text{el}} = \nu_H \phi = \frac{3}{5} \quad (29)$$

in units of the electron charge  $e$ . The most elegant way to see why this happens is by using the Laughlin argument about adding one flux quantum [39] corresponding to the spectral flow [34]. The magnetic flux  $\phi$  threading the antidot is quantized in units of  $h/e$  and the adiabatic increase of  $\phi$  from 0 to 1 transfers electric charge equal to the Hall filling factor  $\nu_H$  from the outer edge to the antidot’s edge [34]. There are only two quasiparticle excitations in the spectrum of the  $\mathbb{Z}_3$  parafermion FQH liquid with electric charge  $3/5$ . If we denote the excitation’s label in the full CFT for the  $\mathbb{Z}_3$  parafermionic states by the weight

$$\underline{\lambda} = l\underline{e}_1^* + \underline{\Delta}_\mu + \underline{\Delta}_\nu, \quad 0 \leq \mu \leq \nu \leq 2, \quad \text{where } l = \mu + \nu \bmod 3 \quad (30)$$

in the notation of Ref. [16], then the electric charge of this excitation is equal to  $Q_{\text{el}}(\underline{\lambda}) = l/(kM + 2) = l/5$  for  $k = 3$  and  $M = 1$ . Therefore the excitations with which the FQH liquid could respond to the flux threading must have  $l = 3$ . There are only two such excitations which can be characterized by the full RCFT characters, or chiral partition functions (8). As can be seen from Eq. (A.1) in Appendix A of Ref. [35] the first one is characterized by the chiral partition function

$$K_3(\tau, 3\zeta; 15)\text{ch}(\underline{\Delta}_0 + \underline{\Delta}_0)(\tau), \quad (31)$$

i.e.,  $l = 3, \mu = \nu = 0$  in Eq. (30) above and corresponds to the chiral vertex operator

$$: e^{i\frac{3}{\sqrt{15}}\phi(z)} : \Phi(\underline{\Delta}_0 + \underline{\Delta}_0), \quad \text{where } \Phi(\underline{\Delta}_0 + \underline{\Delta}_0) = \mathbb{I} \quad (32)$$

is the parafermion field corresponding to the  $\mathbb{Z}_3$  parafermion vacuum and the chiral boson  $\phi(z)$  in the  $\widehat{u(1)}$  vertex exponent, representing the electric charge part of the RCFT, is normalized by (6). The second excitation which can be localized on

the antidot's edge, in response to the flux threading, is characterized by the chiral partition function [16,35]

$$K_3(\tau, 3\zeta; 15)\text{ch}(\underline{\Lambda}_1 + \underline{\Lambda}_2)(\tau) \quad (33)$$

i.e.,  $l = 3, \mu = 1, \nu = 2$  in Eq. (30) and corresponds to the chiral vertex operator (17) where  $\Phi(\underline{\Lambda}_1 + \underline{\Lambda}_2) = \varepsilon$  is the parafermion field corresponding to the Fibonacci anyon. It is obvious from the explicit list of characters in Eq. (A.1) in Appendix A of Ref. [35] that there are no other  $l, \mu$  and  $\nu$  satisfying the pairing rule given in the right-hand side of Eq. (30).

**Remark:** The  $\mathbb{Z}_3$  pairing rule (7) repeated in (30) in the diagonal coset model is naturally inherited from its Abelian parent. In the framework of the so called Maximally Symmetric Chiral Quantum Hall Lattices, see [16] and references therein, the topological charges of the multielectron-like excitations form an odd integer lattice. The structure of this lattice is almost completely determined by the filling factor  $\nu$ , the maximal symmetry and the locality conditions. The elements in the dual lattice represent the topological charges of quasiparticle excitations. However, in order to separate the  $u(1)$  charges from the neutral degrees of freedom we need to have a direct sum decomposition. The almost unique lattice  $\Gamma$  which is derived in [16], for the filling factor  $\nu = k/(k+2)$  (in our case  $k = 3$ ), is not completely decomposable. Nevertheless, there is a decomposable sublattice  $L \subset \Gamma$  in which the one-dimensional charge lattice is completely separated from the neutral sublattice. Because of the inclusion  $L \subset \Gamma \subset \Gamma^* \subset L^*$ , the topological charges of the various super-selection sectors of the original lattice, which belong to the finite Abelian group  $\Gamma^*/\Gamma$ , form a subgroup of the decomposable group  $L^*/L$ , which is bigger than the physical one. The pairing rule Eq. (3.16) in [16] selects those charges of  $L^*/L$  which belong to the original physical super-selection sectors of  $\Gamma^*/\Gamma \subset L^*/L$ , see . The pairing rule (7) is the descendant of the pairing rule in the Abelian parent after the coset projection is done. That is why the diagonal coset approach to the  $\mathbb{Z}_3$  parafermions is more appropriate for the Fibonacci anyons initialization, like in (33), than the others.

It is worth emphasizing here that the chiral partition functions (31) and (33) are not sums over the entire orbit of the simple current (14) like Eq. (8) because we assume that the antidot is well separated from the outer edge or contacts so that electron tunneling into the edge of the antidot is not expected. If there is electron tunneling into the antidot then the full chiral partition functions would be  $\chi_{-2,2}$  instead of Eq. (31) and  $\chi_{-2,1}$  instead of Eq. (33) in the notation of Eq. (8). This sum in Eq. (8) represents the simple physical observation that, in the thermodynamic limit in which the number of electrons goes to infinity, adding one electron/hole to the edge of the chiral QH sample (a disk), does not change anything in the system and should be a symmetry of all thermodynamic quantities computed in the effective CFT.

The modular  $S$  matrix has well-known transformation properties under the action of the simple currents [26] and as a result the entire orbit under the action of the simple currents has the same  $S$ -matrix elements [27]. Notice also that the quantum dimensions of all parafermion fields in Eq. (31) are 1, and the fields  $\Phi(\underline{\Lambda}_0 + \underline{\Lambda}_0) = \mathbb{I}$ ,  $\Phi(\underline{\Lambda}_1 + \underline{\Lambda}_1) = \psi_1$  and  $\Phi(\underline{\Lambda}_2 + \underline{\Lambda}_2) = \psi_2$  are Abelian (the parafermion currents), while the parafermion fields  $\Phi(\underline{\Lambda}_0 + \underline{\Lambda}_1) = \sigma_1$ ,  $\Phi(\underline{\Lambda}_0 + \underline{\Lambda}_2) = \sigma_2$  and  $\Phi(\underline{\Lambda}_1 + \underline{\Lambda}_2) = \varepsilon$  in Eq. (33) all have quantum dimension  $\delta$  and are non-Abelian. This is the physical explanation of the “coarse-graining” of the fusion rules formulated in Ref. [25].

The process of localization of a quasiparticle represented by the field operators (32) or (17) on the antidot’s edge, in response to piercing the antidot by one quantum of magnetic flux, is stochastic. In some cases the localized quasiparticle from the parafermion point of view would be  $\mathbb{I}$ , in the others it would be  $\varepsilon$  and no other possibilities exist because of the  $\mathbb{Z}_3$  paring rule [16]. Following the alternative interpretation of the quantum dimensions [7], according to which the probability to create anyons of type  $a$  and quantum dimension  $d_a$  in a random process is (see Eq. (9.112) in Ref. [7])

$$p_a = \frac{d_a^2}{D^2}, \quad \text{where} \quad D^2 = \sum_a d_a^2$$

is the total quantum dimension, we expect that the probability to create a Fibonacci anyon  $\varepsilon$  is bigger than that to create the unit  $\mathbb{I}$  because  $p_\varepsilon/p_{\mathbb{I}} = \delta^2 = \delta + 1 \approx 2,618$ .

The topological qubit for quantum computation based on Fibonacci anyons, constructed in the basis (4), can be implemented with 4 antidots, each of which is threaded with one quantum of magnetic flux and in which all quasiparticles localized on the antidots are  $\varepsilon$ . This can be achieved by measuring non-destructively each antidot, as shown in the next Subsection, and if on some of the antidots the edge quasiparticle is  $\mathbb{I}$  the stochastic process of initialization is repeated until an  $\varepsilon$  excitation is registered.

Notice that this initialization of the quantum state with a Fibonacci anyon is simpler than the initialization of the Ising anyon state [21] because in the latter the insertion of one quantum of magnetic flux creates two types of excitations which cannot form coherent superpositions due to their opposite fermionic parity. The problem there is solved if we start with two antidots, then insert one flux quantum through one of the antidot and finally apply small voltage between the two antidots to induce tunneling of a single Ising anyon between the two antidots [21,23]. Here the problem of initialization of the Fibonacci anyon is solved much simpler and easier by selecting only those antidots which contain an  $\varepsilon$  field or, by repeating the process of flux insertion until an  $\varepsilon$  field is obtained, i.e., no tunneling is needed.

## 5.2 Measurement of the Fibonacci anyon

One possibility to detect the Fibonacci anyon on the antidot is to look to the interference patterns in Fabry–Pérot interferometers in the backscattered current shown in Fig. 6. Here the two quantum point contacts (QPC), denoted as QPC<sub>1</sub> and QPC<sub>2</sub>,

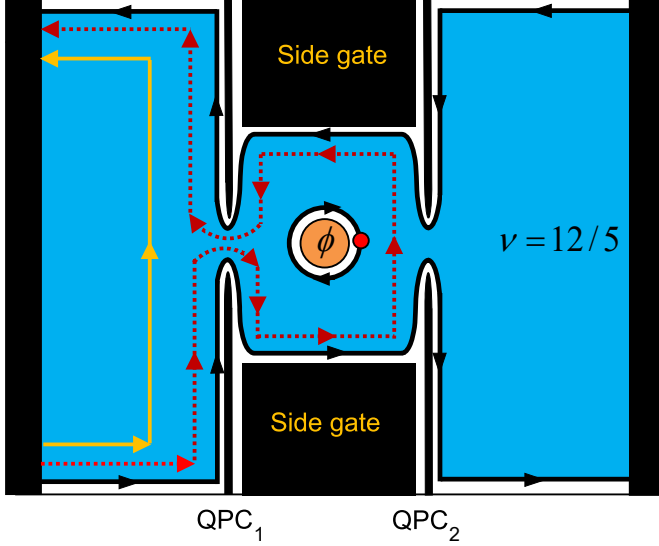


Fig. 6. Measurement of an Fibonacci anyon by Fabri-Perot interferometer

are not completely pinched off and there is a small current reflected back from the interferometer, due to the tunneling of quasiparticles through the QPCs, while almost all electric charge is transmitted through the interferometer along the edge states denoted by arrows in Fig. 6. To lowest order in the amplitudes  $t_1$  and  $t_2$ , for tunneling of fundamental quasiparticles through quantum-point contacts QPC<sub>1</sub> and QPC<sub>2</sub> respectively, the amplitude of the backscattered current of the Fabry–Pérot interferometer shown in Fig. 6, in the quantum state  $|\Psi\rangle$  of the strongly correlated FQH electron system, is proportional to the “diagonal” conductivity [40,27]

$$\begin{aligned} \sigma_{xx} &\propto \|(t_1 U_1 + t_2 U_2) |\Psi\rangle\|^2 = \langle \Psi | (t_1^* U_1^\dagger + t_2^* U_2^\dagger) (t_1 U_1 + t_2 U_2) | \Psi \rangle \\ &= |t_1|^2 + |t_2|^2 + 2\text{Re} \left( t_1^* t_2 \langle \Psi | U_1^{-1} U_2 | \Psi \rangle \right). \end{aligned} \quad (34)$$

The matrix element appearing in Eq. (34) of the two unitary operators  $U_1$  and  $U_2$ , each of which represents the quasiparticle evolution in the state  $|\Psi\rangle$  during the process of tunneling through QPC<sub>1</sub> and QPC<sub>2</sub> respectively, determines the interference effects and can be written as [40]

$$\langle \Psi | U_1^{-1} U_2 | \Psi \rangle = e^{i\alpha} \langle \Psi | (B_1)^2 | \Psi \rangle = e^{i\alpha} \langle \Psi | M | \Psi \rangle \quad (35)$$

where  $\alpha$  is an Abelian phase which is a sum of the dynamical phase associated with the unitary evolution of the quasiparticle transported along the full path around the

central region (the island) of the interferometer containing  $n$  fundamental quasiparticles and the topological phase due to the Aharonov–Bohm effect of the electrically charged quasiparticles in the total magnetic field. The expectation value of  $(B_1)^2 \equiv M$  represents only the action of the pure braiding operator taking the traveling quasiparticle around the static quasiparticles localized in the central region. While for Abelian quasiparticle of type  $a$  transported along a complete loop around quasiparticle of type  $b$  this monodromy always satisfies  $|\langle \Psi | M_{ab} | \Psi \rangle| = 1$ , the monodromy expectation value for non-Abelian anyons  $|\langle \Psi | M_{ab} | \Psi \rangle| \leq 1$  and could eventually be 0, which corresponds to no interference at all [41,40].

To the lowest order in the tunneling interference process, the monodromy expectation value for a quantum state  $|\Psi_{ab}\rangle$  of uncorrelated quasiparticles of type  $a$  and  $b$ , can be computed exactly [42] in terms of the modular  $S$  matrix [26] according to

$$\langle \Psi_{ab} | M | \Psi_{ab} \rangle = \frac{S_{ab} S_{00}}{S_{0a} S_{0b}} \quad (36)$$

where  $S_{ab}$  is the matrix element of the modular  $S$  matrix corresponding to the topological charges  $a$  of the quasiparticle being transported along a complete loop around a quasiparticle of topological charge  $b$ , while 0 labels the vacuum sector, i.e., the state without any quasiparticle. Therefore if we know the  $S$  matrix explicitly we can compare all interference patterns corresponding to given types of static quasiparticles localized in the central region of the interferometer trying in this way to extract information about monodromy matrix elements and proving or disproving the emergence of non-Abelian quasiparticles in each experimental setup. We can use the explicit form of the modular  $S$  matrix for the diagonal coset  $\text{PF}_3$  derived in [27], see Eq. (36) there, to calculate the interference terms in the diagonal conductivity. When we apply small voltage between the two QPCs the most relevant quasiparticles  $\sigma_1$  or  $\sigma_2$  will tunnel creating in this way a monodromy transformation around the antidot. If the localized quasiparticle on the antidot is the field (32) then the parafermion (or neutral part of the) monodromy expectation value will be

$$\langle \Psi_{04} | M | \Psi_{04} \rangle = \frac{S_{04} S_{00}}{S_{00} S_{04}} = 1$$

because the parafermion primary field  $\Phi(\underline{\Lambda}_0 + \underline{\Lambda}_1) = \sigma_1$  (the 4-th basis vector of the  $S$  matrix) is transported along a closed loop around the parafermion primary field  $\Phi(\underline{\Lambda}_0 + \underline{\Lambda}_0) = \mathbb{I}$  (the 4-th basis vector of the  $S$  matrix). If on the other hand the localized quasiparticle on the antidot is the field (17) then the parafermion (or neutral part of the) monodromy expectation value will be

$$\langle \Psi_{64} | M | \Psi_{64} \rangle = \frac{S_{64} S_{00}}{S_{06} S_{04}} = -\frac{1}{\delta^2}$$

because the parafermion primary field  $\Phi(\underline{\Lambda}_0 + \underline{\Lambda}_1) = \sigma_1$  (the 4-th basis vector

of the  $S$  matrix) is transported along a closed loop around the parafermion primary field  $\Phi(\underline{\Lambda}_1 + \underline{\Lambda}_2) = \varepsilon$  (the 6-th basis vector of the  $S$  matrix). Therefore if the Anyon localized on the antidot is Abelian - there is no suppression of the interference term; if the anyon is non-Abelian - there is a suppression of the interference term by a factor of  $1/\delta^2 \approx 0,38$ . The same result is obtained if the tunneling quasiparticle between the QPCs is  $\sigma_2$ .

Notice that this measurement does not change or destroy the state of the anyon on the antidot. So with every antidot we repeat the initialization step of adding one flux quantum inside the antidot, measuring non-destructively the state of the anyon and starting over until the interference suppression is measured and then we can be sure that the anyon localized on the anyon is non-Abelian. In this way we can arrange a topological quantum register of  $n$  Fibonacci anyons. We can use the same type of interferometric measurement to determine the overall topological charge of the register, i.e., whether the register of  $n$  Fibonacci anyons belongs to the CFT representation with  $|\Lambda\rangle = |\mathbb{I}\rangle$  or with  $|\Lambda\rangle = |\varepsilon\rangle$  as discussed in Sect. 4.

### 5.3 *Measurement of the Fibonacci qubit*

This is the same non-destructive measurement like in the previous Subsection, however this time applied to pairs of Fibonacci anyons localized on neighboring antidots. Using our encoding scheme in Eq. (4), if the qubit is in the state  $|0\rangle$ , then the two  $\varepsilon$  fields are in the fusion channel of the identity  $\mathbb{I}$  so there will be no interference suppression. However, if the qubit is in the state  $|1\rangle$ , i.e., the two  $\varepsilon$  fields are in the fusion channel of  $\varepsilon$  then there will be suppression of the interference term by a factor of  $\delta^2$ .

### 5.4 *$n$ -qubit encoding scheme*

In Topological Quantum Computation we intend to encode information in the fusion channels of pairs of Non-Abelian anyons [6,7,8]. Because the Fibonacci anyons  $\varepsilon$  have two fusion channels the encoding scheme could be the same as that for the Ising anyons [21,23]. In this Subsection we will show that it is possible to construct a  $n$ -qubit topological register with  $2n + 2$  Fibonacci anyons (17), i.e., each qubit is realized by a pair of anyons. Each anyon is localized on an antidot by the flux threading procedure described in Sect. 5.1. The state of each qubit is determined by the fusion channel of the pair of Fibonacci anyons, i.e., if the pair fuses to the identity  $\mathbb{I}$  the state of the qubit is  $|0\rangle$  while if the pair fuses to the Fibonacci anyon  $\varepsilon$  the state of the qubit is  $|1\rangle$ . Furthermore, because we would like to represent the multi-anyon coordinate wave function as a CFT correlation function as described in Sect. 4 we need to include one more pair of anyons in order to guarantee that the CFT correlators are non-zero, just like in the Ising TQC. This encoding scheme

is shown in Fig. 7. The register is arranged so that the first and the last anyons are

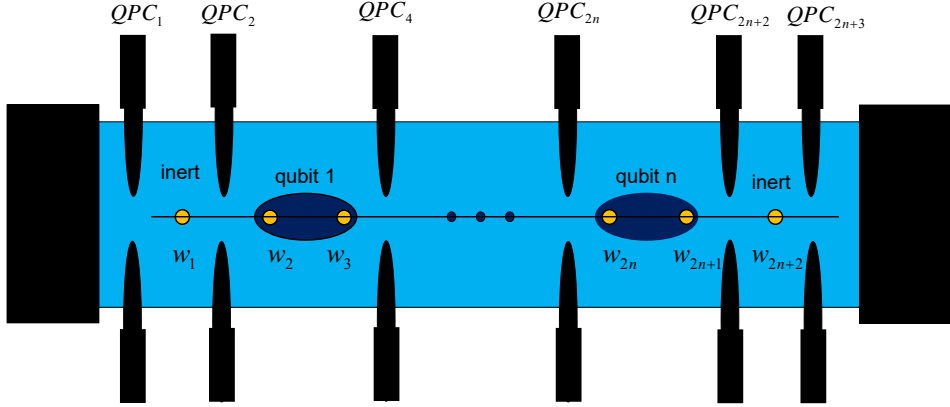


Fig. 7.  $n$ -qubit encoding scheme with  $2n + 2$  Fibonacci anyons. The yellow disks denote the Fibonacci anyons with coordinate  $w_i$  localized on antidots (not shown). There are QPCs between each two neighboring anyons, which can be used for manipulation, however those between the anyons forming a qubit (dark blue ellipses) are not shown. The first and the last anyons are inert and the information is encoded into the  $n$  pairs of anyons between them.

“inert” because they act over the CFT vacuum (left and right) and create definite states under the state-field correspondence [26]. Then the first qubit is formed by the anyons with coordinates  $w_2$  and  $w_3$ . The  $n$ -th qubit is formed by the anyons with coordinates  $w_{2n}$  and  $w_{2n+1}$  and the last anyon carries no information. There are QPCs between each two neighboring qubits so that the state of any qubit can be measured by the diagonal conductance interferometry as discussed in Sect. 5.2.

The computational basis for  $n$ -qubits can be expressed in terms of the CFT correlation functions (or more precisely, the conformal blocks) with  $2n + 2$  fields  $\varepsilon$ , with coordinates  $w_i$  ( $i = 1, \dots, 2n + 2$ ) and  $3r$  parafermion fields  $\psi_1$  (which we will skip from the expression)

$$|\alpha_1 \alpha_2 \dots \alpha_n\rangle = \langle \varepsilon | \varepsilon(w_2) \Pi_{\alpha_1} \varepsilon(w_3) \Pi_1 \varepsilon(w_4) \Pi_{\alpha_2} \varepsilon(w_5) \Pi_1 \dots \Pi_1 \varepsilon(w_{2n}) \Pi_{\alpha_n} \varepsilon(w_{2n+1}) | \varepsilon \rangle, \quad (37)$$

where  $\alpha_i = 0$  corresponds to the fusion channel  $\varepsilon \times \varepsilon = \mathbb{I}$ , while  $\alpha_i = 1$  corresponds to the fusion channel  $\varepsilon \times \varepsilon = \varepsilon$ . The rule is that every even in order projector [24] is  $\Pi_1$ , which corresponds to the odd numbers of  $\varepsilon$  in the Bratteli diagrams, such as those in Fig. 4 and Fig. 8. Graphically the Bratteli diagrams corresponding to the computational basis include two consecutive horizontal lines (double ropes) on level  $\varepsilon$  and two consecutive ropes (pails) one from level  $\varepsilon$  to level  $\mathbb{I}$  and the second from level  $\mathbb{I}$  to level  $\varepsilon$ . The notation of the computational basis states is the following: from left to right we write 0 for a pail and 1 for double ropes. The rest of the CFT blocks which contain odd number of horizontal ropes at level  $\varepsilon$  are Non-Computational states. The logic behind this rule is that we look for a scalable



qubit encoding scheme for any  $n$ . Since one qubit in the state  $|1\rangle$  is formed by 2 horizontal ropes on level  $\varepsilon$ , as can be seen from Fig. 4, there is no way to obtain computational states with odd number of horizontal ropes for multiple qubits.

We shall assume that we can implement the quantum gates by braiding of Fibonacci anyons. The practical execution of the braiding is beyond the scope of this paper. What is important for us is that the elementary generators  $B_i$ , ( $i = 1, \dots, n-1$ ) representing the braiding of the  $i$ -th anyon with  $i+1$ -th can be derived from the coordinate wave functions and must satisfy the Artin's relations for the generators of  $\mathcal{B}_n$

$$\begin{aligned} B_i B_j &= B_j B_i, & \text{for } |i-j| \geq 2 \\ B_i B_{i+1} B_i &= B_{i+1} B_i B_{i+1}, & \text{where } B_i = R_{i,i+1} \in \mathcal{B}_n. \end{aligned} \quad (38)$$

We shall start in the next section with the one-qubit gates.

## 6 Single-qubit gates

As we have seen in Eq. (4) the dimension of the one-qubit space realized in terms of CFT correlators with 4  $\varepsilon$  fields is 2, as it should be for the one-qubit system. In Eq. (19) we have constructed the 4-anyon wave function in terms of the parafermion CFT correlation function with 4  $\varepsilon$  fields and  $N = 3r$  electron fields with  $r$  integer. The  $u(1)$  factors of the wave function are of Laughlin type and are written explicitly.

The remaining parafermion CFT correlation function in Eq. (19) was computed in Ref. [25]. Following the explicit construction in Ref. [16] of the quasiparticle wavefunctions for the  $\mathbb{Z}_k$  parafermion FQH states as symmetrization of Laughlin quasiparticle wavefunctions in an Abelian parent CFT the authors of Ref. [25] were able to compute the parafermion wave function with 4  $\varepsilon$  fields in terms of the hypergeometric function using the original results of Knizhnik and Zamolodchikov [43]. This 4  $\varepsilon$  CFT correlation function is not appropriate for our physical implementation of the Fibonacci TQC because as we can see in Eq. (19) there must be also  $N = 3r$  ( $r$  is a big positive integer) parafermion fields  $\psi_1$ . Using the approach of Refs. [16] and [25] the result for general  $r$  has been derived in Ref. [24] and is explicitly shown in Eqs. (22)–(27) above.

Now that we have the explicit coordinate wave functions for 4 Fibonacci anyons (17) and  $N$  electron fields (14) we can derive the braid generators  $B_a^{(4)}$  by analytic continuation ( $w_a - w_{a+1}$ )  $\rightarrow e^{i\pi}(w_a - w_{a+1})$  of the wave functions. The result is

obtained in Ref. [24] and we summarize it as follows:

$$B_1^{(4)} = \begin{bmatrix} q^{-1} & 0 \\ 0 & -q \end{bmatrix}, \quad B_2^{(4)} = \begin{bmatrix} q^{-3}\tau & \sqrt{\tau} \\ \sqrt{\tau} & -q^3\tau \end{bmatrix}, \quad B_3^{(4)} = B_1^{(4)} \quad (39)$$

where  $q = e^{i\pi/5}$  and  $\tau = 1/\delta$  is the inverse of the golden ratio  $\delta$  defined after Eq. (1). Notice that our braid generators for  $4\varepsilon$  functions differ from those of Ref. [24] by a factor of  $q^3$  which comes from the Laughlin-type factors  $(w_a - w_b)^{3/5}$  in Eq. (19) after making the analytic continuation  $(w_a - w_b) \rightarrow e^{i\pi}(w_a - w_b)$  when braiding  $w_a$  with  $w_b$ . It is not difficult to check [24] that the braid generators (39) of the braid group  $\mathcal{B}^{(4)}$  satisfy the Artin's relations (38).

It is important to emphasize one of the findings in Ref. [25] which has been confirmed in Ref. [24]: it follows from the explicit form of the  $4\varepsilon$  function that the 3-point correlation functions of the  $\varepsilon$  is zero, i.e., the operator product expansion coefficient is  $C_{\varepsilon\varepsilon}^\varepsilon = 0$ . However, the operator product expansion of the  $\varepsilon$  field is still non-Abelian

$$\begin{aligned} \varepsilon(w_1)\varepsilon(w_2) \underset{w_1 \rightarrow w_2}{\simeq} & \frac{1}{w_{12}^{4/5}} + \frac{0}{w_{12}^{2/5}}\varepsilon(w_2) + \sqrt{\frac{12C}{7}}w_{12}^{3/5}\varepsilon'(w_2), \\ 2C & = \sqrt{\frac{\Gamma(\frac{1}{5})\Gamma^3(\frac{3}{5})}{\Gamma(\frac{4}{5})\Gamma^3(\frac{2}{5})}} \end{aligned} \quad (40)$$

where  $\varepsilon'(w_2)$  is another Virasoro primary field with CFT dimension  $\Delta' = 7/5$ . This field  $\varepsilon'$  is in the same topological sector as  $\varepsilon$ , which is described by the parfermion character  $\text{ch}(\underline{\Lambda}_1 + \underline{\Lambda}_2)$ , has the same electric properties however  $\varepsilon'$  is already a true Fibonacci anyon. This peculiarity does not change our encoding scheme, because we encode information in the fusion channel of pairs of non-Abelian anyons—whether the anyons fuse to  $\varepsilon$  or to  $\varepsilon'$  is not important. What is important is that there are two fusion channels - one with quantum dimension 1 and one with quantum dimension  $\delta$  and this allows us to construct a qubit. From the point of view of the qubit initialization  $\varepsilon'$  is not a problem because whenever we create  $\varepsilon$  on the antidot the field  $\varepsilon'$  is created as well.

The generators  $B_1^{(4)}$  and  $B_3^{(4)}$  of the braid group  $\mathcal{B}^{(4)}$  are diagonal and therefore they can be obtained directly from the OPE (40). The generator  $B_2^{(4)}$  is not diagonal in the basis  $(\Phi^{(0)}, \Phi^{(1)})$  defined in Eqs. (24) and (25), however, as has been proven in Ref. [24] this matrix is diagonal in the *dual basis*  $(\Theta^{(0)}, \Theta^{(1)})$ , which determines the behavior of the hypergeometric functions when  $\eta \sim 1$  (or,  $1 - \eta \sim 0$ ). Remarkably enough, the two bases are simply related

$$\begin{bmatrix} \Theta^{(0)} \\ \Theta^{(1)} \end{bmatrix} = F \begin{bmatrix} \Phi^{(0)} \\ \Phi^{(1)} \end{bmatrix}, \quad \text{where} \quad F = \begin{bmatrix} \tau & \sqrt{\tau} \\ \sqrt{\tau} & -\tau \end{bmatrix} \quad (41)$$

is the  $F$  matrix of Preskill (without any phase on the off-diagonal) [7]. The result in Eq. (41) obtained in Ref. [24] uses the well-known transformation properties of the hypergeometric functions [38]. Summarizing the results of Ref. [24] the braid generator  $B_2^{(4)}$  is diagonal in the dual basis (41) and has the same eigenvalues as  $B_1^{(4)}$ , i.e.,  $B_2^{(4)} = FB_1^{(4)}F$ . Notice that this result describes the braiding of 4 Fibonacci anyons in the CFT correlation functions including  $N \gg 1$  electron fields, generalizing in a non-trivial way the case  $N = 0$  derived in Ref. [25].

It is known that the representations of the type (39) of the braid group  $\mathcal{B}^{(4)}$  for braiding 4 Fibonacci anyons are dense within the unitary group  $U(2)$  [7,8]. This means that any single-qubit gate can be implemented by products of  $B_i^{(4)}$  and their inverses with an arbitrary precision. Using the Solovay–Kitaev algorithm [3] the Hadamard gate can be constructed approximately with 30 weaves with an error less than 0.00657 [19,44].

$$\begin{aligned} \tilde{H} &= B_1^4 B_2^{-2} B_1^2 B_2^{-2} B_1^2 B_2^2 B_1^{-2} B_2^4 B_1^2 B_2^{-2} B_1^{-2} B_2^2 B_1^2 = \\ & \frac{i}{\sqrt{2}} \begin{bmatrix} 1.00402 + 0.00555i & 0.99594 - 0.004772i \\ 0.995937 + 0.00477i & -1.00402 + 0.00555i \end{bmatrix} \simeq iH, \end{aligned} \quad (42)$$

where we have skipped the superscript (4) of  $B_i^{(4)}$  for simplicity, the negative powers of the matrices are the positive powers of the inverse matrices, and for the error we have used the matrix norm function (i.e., the square root of the maximum eigenvalue of  $AA^\dagger$ ) implemented in Maple

$$\text{MatrixNorm}(A, 2) = \sqrt{\max(\text{Eigenvalues}(A.A^\dagger)_j, j = 1, 2)}$$

for  $A = \tilde{H} - iH$ .

The Hadamard gate (42) together with the exact single-qubit  $Z$  gate

$$-Z = \left(B_1^{(4)}\right)^5, \quad HZH = X \quad (43)$$

can be used to approximate to construct an approximation of the single-qubit Pauli- $X$  gate [3]. Below we give a better approximation to the  $iX$  gate with 44 weaves and accuracy  $8.6 \times 10^{-4}$  taken from [18]

$$\begin{aligned} i\tilde{X} &= B_1^{-2} B_2^{-2} B_1^2 B_2^{-2} B_1^2 B_2^{-4} B_1^2 B_2^4 B_1^{-2} B_2^4 B_1^{-2} B_2^2 B_1^2 B_2^{-2} B_1^4 B_2^{-4} B_1^{-2} = \\ & \begin{bmatrix} 0.0006 - 0.0002i & -0.0006 + 1.i \\ 0.0006 + 1.i & 0.0006 + 0.0002i \end{bmatrix} \simeq iX. \end{aligned} \quad (44)$$

Next, the  $T$  gate (or  $\pi/8$  gate) [3] can be approximated upto phase with 14 weaves with accuracy  $3.3 \times 10^{-2}$  as follows

$$\begin{aligned} \tilde{T} &= B_1^{-2} B_2 B_1^{-2} B_2 B_1^{-1} B_2 B_1^{-1} B_2 B_1^{-2} B_2 = \\ &\begin{bmatrix} 1. + 0.i & 0.0317 + 0.0025i \\ -0.0242 - 0.0207i & 0.7055 + 0.7087i \end{bmatrix} \simeq T. \end{aligned} \quad (45)$$

Some other examples of single-qubit gates are the Pauli  $Y$  gate with 45 weaves and accuracy  $8.6 \times 10^{-4}$  taken from [18]

$$\begin{aligned} \tilde{Y} &= B_1^2 B_2 B_1^{-2} B_2 B_1^{-2} B_2^4 B_1^{-2} B_2^4 B_1^2 B_2^{-4} B_1^2 B_2^{-4} B_1^2 B_2^{-2} B_1^{-2} B_2^2 B_1^{-4} B_2^4 B_1^{-3} = \\ &\begin{bmatrix} -0.0006 - 0.0002i & -0.0006 - 1.i \\ -0.0006 + 1.i & 0.0006 - 0.0002i \end{bmatrix} \simeq Y, \end{aligned} \quad (46)$$

the  $-H$  gate (improved over [44]) with 27 weaves and accuracy  $4.8 \times 10^{-3}$  taken from [?]

$$\begin{aligned} -\tilde{H} &= B_1^3 B_2 B_1^{-2} B_2^{-1} B_1^{-4} B_2 B_1^{-1} B_2 B_1^{-3} B_2 B_1^{-1} B_2 B_1^{-1} B_2 B_1^{-2} B_2 B_1^{-1} = \\ &\begin{bmatrix} -0.7053 - 0.003i & -0.7089 - 0.0029i \\ -0.7089 + 0.0029i & 0.7053 - 0.003i \end{bmatrix} \simeq -H, \end{aligned} \quad (47)$$

and the  $S$  gate multiplied by the phase  $q$  with 31 weaves and accuracy  $1.2 \times 10^{-2}$

$$\begin{aligned} \tilde{qS} &= B_2^{-3} B_1^{-4} B_2 B_1^3 B_2^{-4} B_1^4 B_2^5 B_1^{-3} B_2^{-3} = \\ &\begin{bmatrix} 0.7085 + 0.7056i & 0.0059 - 0.0098i \\ 0.0059 + 0.0098i & -0.7085 + 0.7056i \end{bmatrix} \simeq qS. \end{aligned} \quad (48)$$

Another important exact gate is the  $F$  gate in Eq. (41) (upto a minus sign) which can be implemented by braiding as follows

$$B_1^{(4)} B_2^{(4)} B_1^{(4)} = -F. \quad (49)$$

## 7 Two-qubit gates

The two-qubit topological register can be realized with 6 Fibonacci anyons. However, the dimension of the Hilbert space with 6 anyons with total quantum dimension 1 is 5 as can be seen from Fig. (1) while the dimension of the two-qubit states is 4. Following the general qubit encoding scheme described in Sect. 5.4 we denote the fusion channel of each pair of Fibonacci anyons as a subscript to the parentheses defining the pair and give below the notation for all possible fusion-path states with 6 Fibonacci anyons

$$\begin{aligned} |00\rangle &= \langle \varepsilon | (\varepsilon\varepsilon)_{\mathbb{I}} (\varepsilon\varepsilon)_{\mathbb{I}} | \varepsilon \rangle \\ |01\rangle &= \langle \varepsilon | (\varepsilon\varepsilon)_{\mathbb{I}} (\varepsilon\varepsilon)_{\varepsilon} | \varepsilon \rangle \end{aligned}$$

$$\begin{aligned}
|10\rangle &= \langle \varepsilon | (\varepsilon\varepsilon)_\varepsilon (\varepsilon\varepsilon)_\mathbb{I} | \varepsilon \rangle \\
|11\rangle &= \langle \varepsilon | (\varepsilon\varepsilon)_\varepsilon (\varepsilon\varepsilon)_\varepsilon | \varepsilon \rangle \\
|NC\rangle &= \langle \varepsilon | \varepsilon (\varepsilon\varepsilon)_\mathbb{I} \varepsilon | \varepsilon \rangle.
\end{aligned} \tag{50}$$

Now it is obvious that in addition to the computational basis for two qubits there is another possible fusion-path state which we denote as  $|NC\rangle$  as an additional state outside our computational space which we will call a Non-Computational state. What we need for TQC are the first 4 states denoted  $\{|00\rangle, |01\rangle, |10\rangle, |11\rangle\}$ . However, as we shall see later, it is possible for some combination of elementary braids to arrive at the state  $|NC\rangle$  (e.g., when braiding the anyons with coordinates  $w_3$  and  $w_4$ ) which will be leakage of information outside the computational space. This needs special attention when braiding the 6 Fibonacci anyons.

It is possible and very convenient to represent the fusion-path states by the corresponding Bratteli diagrams, as shown in Fig. 8. It is obvious that when the arrow at the step with  $2\varepsilon$  fields reaches the horizontal axis then the corresponding state of the first qubit is  $|0\rangle$ , while if it reaches the dotted line of  $\varepsilon$  then the state of the first qubit is  $|1\rangle$ . Similarly, if the composition of the second pair of  $\varepsilon$  fields reaches at the step with  $4\varepsilon$  fields the horizontal axis then the corresponding state of the second qubit is  $|0\rangle$ , while if it reaches the dotted line of  $\varepsilon$  then the state of the second qubit is  $|1\rangle$ . The representation of the generators of the braid group  $\mathcal{B}^{(6)}$  have been obtained in Ref. [24] (in an appropriate basis which differs from the computational one (50) by simple reordering) by fusing some of the Fibonacci anyons before braiding, which leads to a direct-sum decomposition into into braid generators with  $n = 4$  (with dimension 2) and  $n = 5$  (with dimension 3). The 5 braid generators of  $\mathcal{B}^{(6)}$  in the basis (50) can be written as follows [24]:

$$\begin{aligned}
B_1^{(6)} &= \begin{bmatrix} q^{-1} & 0 & 0 & 0 & 0 \\ 0 & q^{-1} & 0 & 0 & 0 \\ 0 & 0 & -q & 0 & 0 \\ 0 & 0 & 0 & -q & 0 \\ 0 & 0 & 0 & 0 & -q \end{bmatrix}, \quad B_2^{(6)} = \begin{bmatrix} B_{11} & 0 & B_{12} & 0 & 0 \\ 0 & B_{11} & 0 & B_{12} & 0 \\ B_{21} & 0 & B_{22} & 0 & 0 \\ 0 & B_{21} & 0 & B_{22} & 0 \\ 0 & 0 & 0 & 0 & -q \end{bmatrix}, \\
B_3^{(6)} &= \begin{bmatrix} q^{-1} & 0 & 0 & 0 & 0 \\ 0 & -q & 0 & 0 & 0 \\ 0 & 0 & -q & 0 & 0 \\ 0 & 0 & 0 & B_{11} & B_{12} \\ 0 & 0 & 0 & B_{21} & B_{22} \end{bmatrix}, \quad B_4^{(6)} = \begin{bmatrix} B_{11} & B_{12} & 0 & 0 & 0 \\ B_{21} & B_{22} & 0 & 0 & 0 \\ 0 & 0 & B_{11} & B_{12} & 0 \\ 0 & 0 & B_{21} & B_{22} & 0 \\ 0 & 0 & 0 & 0 & -q \end{bmatrix}, \\
B_5^{(6)} &= \begin{bmatrix} q^{-1} & 0 & 0 & 0 & 0 \\ 0 & -q & 0 & 0 & 0 \\ 0 & 0 & q^{-1} & 0 & 0 \\ 0 & 0 & 0 & -q & 0 \\ 0 & 0 & 0 & 0 & -q \end{bmatrix}, \tag{51}
\end{aligned}$$

where  $B_{ij}$  with  $i, j = 1, 2$  are the matrix elements of  $B_2^{(4)}$  defined in Eq. (39).

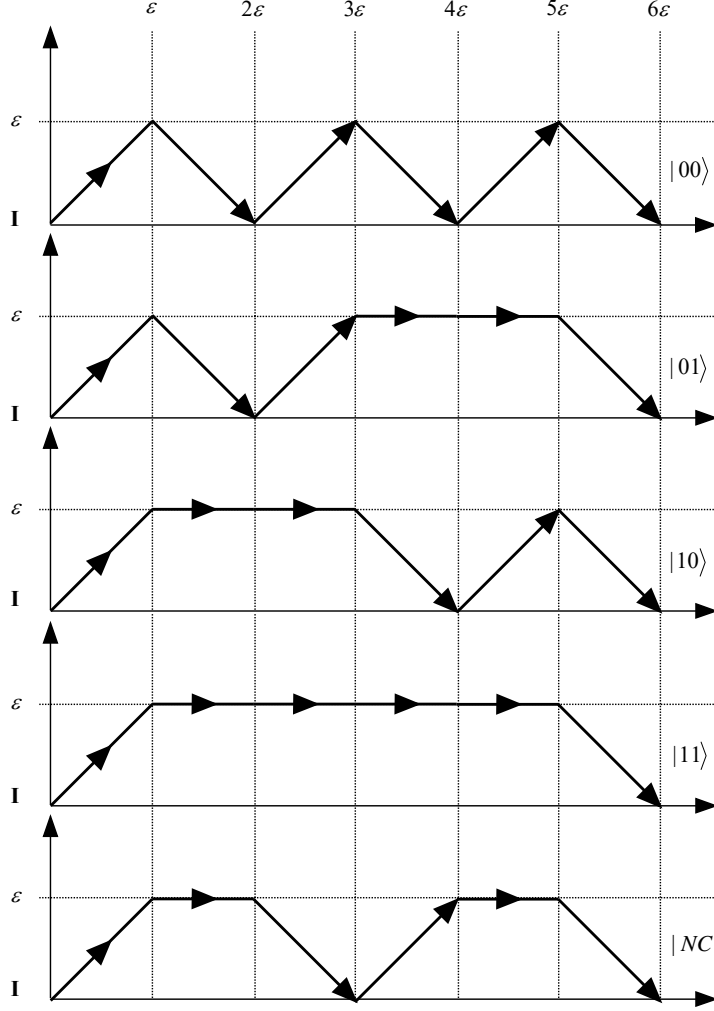


Fig. 8. Bratteli diagrams for the 4 states in the computational basis  $\{|00\rangle, |01\rangle, |10\rangle, |11\rangle\}$  and the non-computational state  $|NC\rangle$ , of 6 Fibonacci anyons with total topological charge  $\mathbb{I}$  (denoted by  $\mathbf{I}$  in the figure).

Obviously, the braid generator  $B_3^{(6)}$  mixes the state  $|11\rangle$  from the computational basis with the non-computational state  $|NC\rangle$  which may lead to information leakage and loss of unitarity. One possible solution to the problem of potential information leakage is one or two of the  $\varepsilon$  fields, e.g., the inert anyons to be excluded from the braiding in order to reduce the space dimension [19].

Notice that the matrices  $R := B_1^{(4)}$  and  $B := B_2^{(4)}$  which can be used to approximate with arbitrary precision any operation from  $SU(2)$  for a single qubit can be embedded into the two-qubit system by

$$\begin{aligned}
B_1^{(6)} &= (R \otimes \mathbb{I}_2) \oplus (-q), & B_2^{(6)} &= (B \otimes \mathbb{I}_2) \oplus (-q), \\
B_4^{(6)} &= (\mathbb{I}_2 \otimes B) \oplus (-q), & B_5^{(6)} &= (\mathbb{I}_2 \otimes R) \oplus (-q).
\end{aligned} \tag{52}$$

This means that any single-qubit operation can be implemented in exactly the same way in the two-qubit system. This also means that 4 of the 5 generators of the group  $\mathcal{B}^{(6)}$  are not entangling, because they act as  $\mathbb{I}_2$  on one of the qubits, and the only entangling generator might be  $B_3^{(6)}$ .

Two important exact two-qubit gates are the embeddings of the single-qubit  $F$  gate into a two-qubit system

$$\begin{aligned}
F_1 &= B_1^{(6)} B_2^{(6)} B_1^{(6)} = -(F \otimes \mathbb{I}_2) \oplus q^{-3} \\
F_2 &= B_5^{(6)} B_4^{(6)} B_5^{(6)} = -(\mathbb{I}_2 \otimes F) \oplus q^{-3}
\end{aligned} \tag{53}$$

## 8 Three-qubit gates

The topological register containing three qubits should have dimension 8 and, at first glance, could eventually be realized with 7 Fibonacci anyons because the dimension of the fusion-path states is exactly 8. However, following the construction of one and two qubits by encoding the information in the fusion channel of pairs of Fibonacci anyons it is necessary to use 8 anyons fusing altogether to the vacuum. Thus the quantum information encoding is as follows: if the  $l$ -th pair of Fibonacci anyons fuse to  $\mathbb{I}$  (i.e., the fusion path at position  $2l\varepsilon$  touches the horizontal axis in Figure 9) then the corresponding quantum bit is  $|0\rangle$ , while if they fuse to the  $\varepsilon$  (i.e., the fusion path at position  $2l\varepsilon$  touches the  $\varepsilon$  dashed line in Figure 9) then the corresponding quantum bit is  $|1\rangle$ . However, the space of the fusion-path states for wavefunctions containing 8 Fibonacci anyons is bigger than the space spanned by the states shown in Figure (9). Its dimension is 13 as can be seen from Fig. 1 and hence there are 5 additional basis vectors which will not participate in the TQC scheme and we will again call them non-computational, see Fig. 10 where their fusion-paths are shown. As can be seen from Fig. 9 the three-qubit computational basis can also be labeled by the different ways to represent the number 8 as sums of even positive integers bigger than 1. For example the first computational state  $|000\rangle$  can be labeled as  $|2 + 2 + 2 + 2\rangle$  because the horizontal lengths of the fusion paths connecting two successive points on the horizontal axis are  $2 + 2 + 2 + 2 = 8$  and the order of the paths is important.

Similarly the non-computational states can be labeled by the different possible ways to represent the number 8 as sums of even and odd numbers bigger than 1, see Fig. 10. For example the first non-computational state is labeled by  $2 + 3 + 3$  because the lengths of the fusion paths connecting two successive points on the

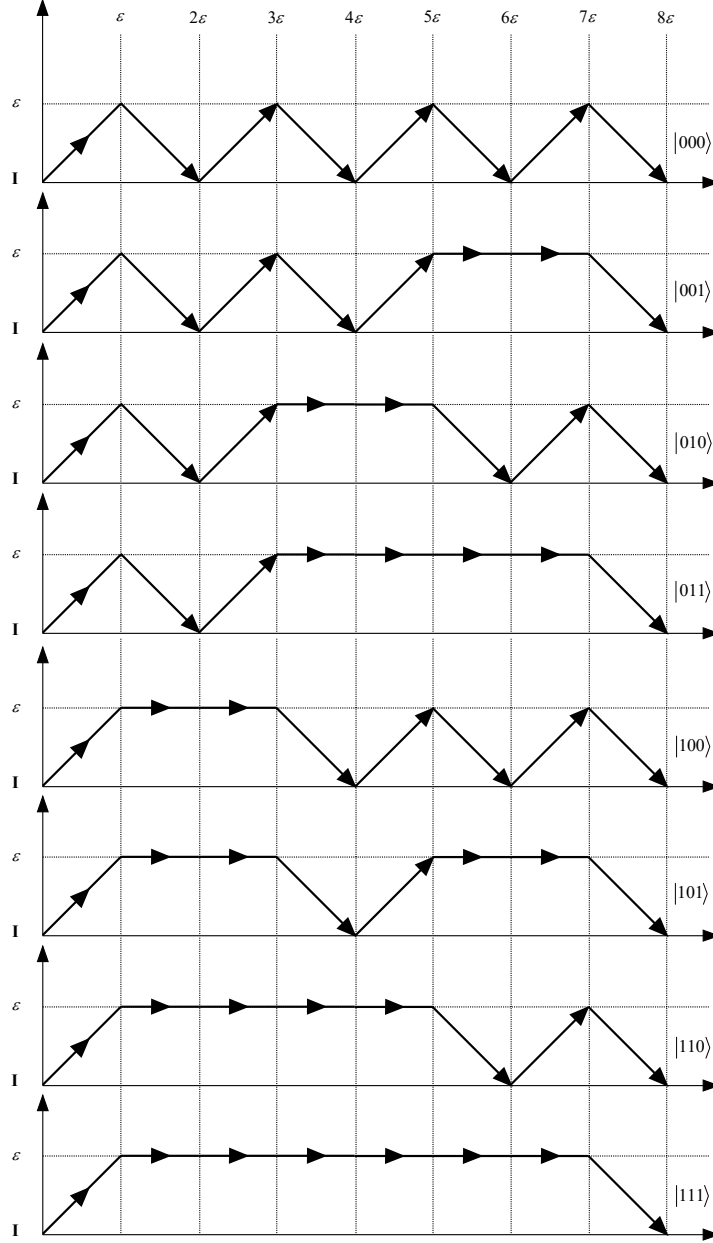


Fig. 9. Bratteli diagrams for the 8 states in the computational basis  $\{|000\rangle, |001\rangle, |010\rangle, |011\rangle, |100\rangle, |101\rangle, |110\rangle, |111\rangle\}$  of 8 Fibonacci anyons with total topological charge  $\mathbb{I}$  (denoted by  $\mathbf{I}$  in the figure).

horizontal axis are  $2 + 3 + 3 = 8$  and the order of the paths are important. It is worth emphasizing that all non-computational states in the Bratteli diagrams in Fig. 10, as well as the two-qubit state  $|NC\rangle$ , contain an odd number of horizontal arrows along the dotted horizontal line at level  $\varepsilon$  which is impossible to achieve in the qubit encoding scheme given in Fig. 4. This is why all these states are non-computational.

The generators of the braid group  $\mathcal{B}^{(8)}$  could be expressed recursively in terms of



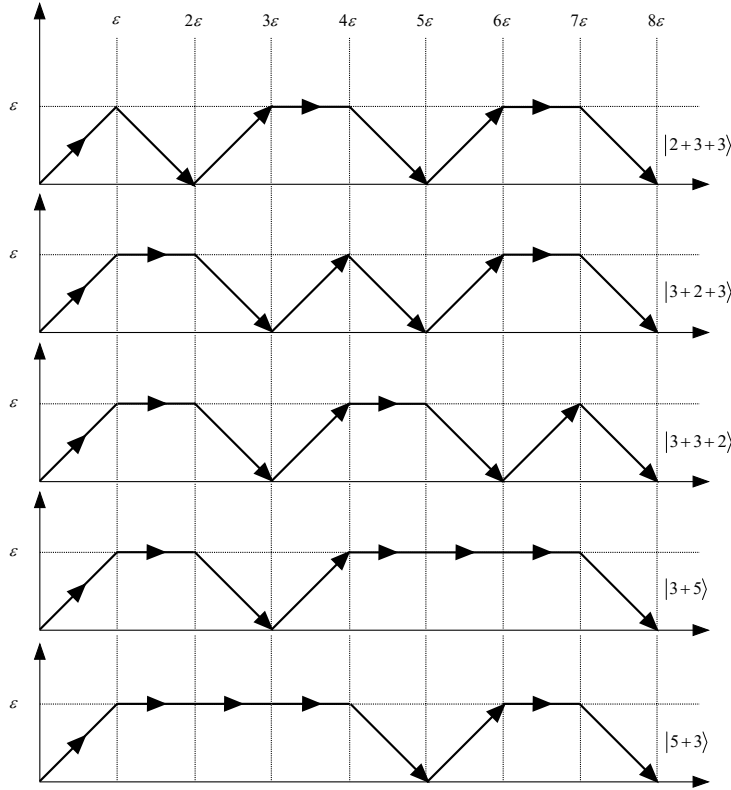


Fig. 10. Bratteli diagrams for the 5 non-computational states of 8 Fibonacci anyons with total topological charge  $\mathbb{I}$  (denoted by  $\mathbf{I}$  in the figure) labeled by the different possible ways to represent the number 8 as sums of even and odd numbers bigger than 1.

the generators of the braid group  $\mathcal{B}^{(6)}$  and  $\mathcal{B}^{(7)}$ . To see this recall that if we fuse the last two  $\varepsilon$  fields we obtain either  $\mathbb{I}$  or  $\varepsilon$ . Therefore the correlation function becomes either a topological register with 6 anyons or such a register with 7 anyons. In order to derive them we will use a more convenient ordering of the 8 computational states shown in Fig. 9 and 5 non-computational states shown in Fig. 10, i.e.,

$$\begin{aligned}
 &|000\rangle, |100\rangle, |3+3+2\rangle, |010\rangle, |110\rangle, |3+2+3\rangle, |2+3+3\rangle, \\
 &|5+3\rangle, |001\rangle, |101\rangle, |3+5\rangle, |011\rangle, |111\rangle.
 \end{aligned} \tag{54}$$

This ordering is such that, if we fuse the last two Fibonacci anyons, the first 5 states form a representation of the  $n = 6$  while the second 8 states form a representation of  $n = 7$ . Now it is not difficult to find that all braid generators in the basis (54), except for the last two, are direct sums of the generators of  $\mathcal{B}^{(6)}$  and  $\mathcal{B}^{(7)}$ , i.e.,

$$B_i^{(8)} = B_i^{(6)} \oplus B_i^{(7)}, \quad i = 1, \dots, 5, \tag{55}$$

which is a remarkable manifestation of the Fibonacci numbers, that are the dimen-

sions of the corresponding braid generators. The last two generators are explicitly calculated in Ref. [24] and can be written in the basis (54) as follows

$$B_6^{(8)} = \begin{bmatrix} B_{11}\mathbb{I}_5 & 0 & B_{12}\mathbb{I}_5 \\ 0 & -q\mathbb{I}_3 & 0 \\ B_{21}\mathbb{I}_5 & 0 & B_{22}\mathbb{I}_5 \end{bmatrix}, \quad B_7^{(8)} = \begin{bmatrix} q^{-1}\mathbb{I}_5 & 0 \\ 0 & -q\mathbb{I}_8 \end{bmatrix},$$

where  $\mathbb{I}_3$ ,  $\mathbb{I}_5$  and  $\mathbb{I}_8$  are the unit matrices with dimensions 3, 5 and 8, respectively, and  $B_{ij}$  with  $i, j = 1, 2$  are the matrix elements of  $B_2^{(4)}$  defined in Eq. (39). This recursive derivation of the generators of the braid group  $\mathcal{B}^{(8)}$  is generalized for  $n$  Fibonacci anyons in Ref. [24] where the generators of the braid groups  $\mathcal{B}^{(3)}$ ,  $\mathcal{B}^{(5)}$ ,  $\mathcal{B}^{(7)}$ , etc. are also explicitly calculated.

## Acknowledgements

LSG has been supported as a Research Fellow by the Alexander von Humboldt Foundation. LSG and LH have been supported by the Bulgarian Scientific Fund under Contract No. DN 18/3 (2017). This work has been done under the project BG05M2OP001-1.002-0006 "Quantum Communication, Intelligent Security Systems and Risk Management (QUASAR)" financed by the Operational Program SESG.

## References

- [1] J. P. Dowling and G. J. Milburn, "Quantum technology: the second quantum revolution," *Phil. Trans. R. Soc. A* **361** (2003) 1655–1674.
- [2] L. Jaeger, *The Second Quantum Revolution*. Copernicus Cham, 2018.
- [3] M. Nielsen and I. Chuang, *Quantum Computation and Quantum Information*. Cambridge University Press, 2000.
- [4] A. F. A. K., and R. e. a. Babbush, "Quantum supremacy using a programmable superconducting processor," *Nature* **574** (2019) 505–510.
- [5] Y. W. et al., "Strong quantum computational advantage using a superconducting quantum processor," *Phys. Rev. Lett.* **127** (2021) 180501.
- [6] A. Kitaev, "Fault-tolerant quantum computation by anyons," *Ann. of Phys. (N.Y.)* **303** (2003) 2.
- [7] J. Preskill, "Topological quantum computation," *Lecture Notes for Physics 219* (2004) <http://www.theory.caltech.edu/~preskill/ph219>.

- [8] S. D. Sarma, M. Freedman, C. Nayak, S. H. Simon, and A. Stern, “Non-Abelian Anyons and Topological Quantum Computation,” *Rev. Mod. Phys.* **80** (2008) 1083, arXiv:0707.1889.
- [9] S. H. Simon, *Topological Quantum*. Oxford University Press, Oxford UK, 2023.
- [10] F. Wilczek, *Fractional statistics and anyon superconductivity*. World Scientific, Singapore, 1990.
- [11] G. Moore and N. Read, “Nonabelions in the fractional quantum Hall effect,” *Nucl. Phys.* **B360** (1991) 362.
- [12] K. K. W. Ma, M. R. Peterson, V. W. Scarola, and K. Yang, *Encyclopedia of Condensed Matter Physics*, vol. 1, ch. Fractional quantum Hall effect at the filling factor  $\nu = 5/2$ , pp. 324–365. Elsevier, 2nd ed., 2024.
- [13] A. Ahlbrecht, L. S. Georgiev, and R. F. Werner, “Implementation of Clifford gates in the Ising-anyon topological quantum computer,” *Phys. Rev. A* **79** (2009) 032311, arXiv:0812.2338.
- [14] H. C. Choi, W. Kang, S. D. Sarma, L. N. Pfeiffer, and K. W. West, “Activation gaps of fractional quantum Hall effect in the second Landau level,” *Phys. Rev. B* **77** (2008) 081301.
- [15] N. Read and E. Rezayi, “Beyond paired quantum Hall states: parafermions and incompressible states in the first excited Landau level,” *Phys. Rev. B* **59** (1998) 8084.
- [16] A. Cappelli, L. S. Georgiev, and I. T. Todorov, “Parafermion Hall states from coset projections of Abelian conformal theories,” *Nucl. Phys. B* **599** [FS] (2001) 499–530, hep-th/0009229.
- [17] M. Freedman, M. Larsen, and Z. Wang, “A modular functor which is universal for quantum computation,” *Commun. Math. Phys.* **227** (2002) 605, quant-ph/0001108.
- [18] N. Bonesteel, L. Hormozi, G. Zikos, and S. Simon, “Braid topologies for quantum computation,” *Phys. Rev. Lett.* **95** (2005) 140503.
- [19] L. Hormozi, G. Zikos, N. E. Bonesteel, and S. H. Simon, “Topological quantum compiling,” *Phys. Rev. B* **75** (2007) 165310.
- [20] L. Hormozi, N. Bonesteel, and S. Simon, “Topological quantum computing with Read–Rezayi states,” *Phys. Rev. Lett.* **103** (2009) 160501.
- [21] S. D. Sarma, M. Freedman, and C. Nayak, “Topologically-protected qubits from a possible non-Abelian fractional quantum Hall state,” *Phys. Rev. Lett.* **94** (2005) 166802, cond-mat/0412343.
- [22] L. S. Georgiev, “Topologically protected gates for quantum computation with non-Abelian anyons in the Pfaffian quantum Hall state,” *Phys. Rev. B* **74** (2006) 235112, cond-mat/0607125.

- [23] L. S. Georgiev, “Towards a universal set of topologically protected gates for quantum computation with Pfaffian qubits,” *Nucl. Phys.* **B 789** (2008) 552–590, hep-th/0611340.
- [24] L. Hadjiivanov and L. S. Georgiev, “Braiding Fibonacci anyons,” arXiv:2404.01778.
- [25] E. Ardonne and K. Schoutens, “Wavefunctions for topological quantum registers,” *Ann. Phys.* **322** (2007) 201–235.
- [26] P. Di Francesco, P. Mathieu, and D. Sénéchal, *Conformal Field Theory*. Springer–Verlag, New York, 1997.
- [27] L. S. Georgiev, “Exact Modular  $S$  Matrix for  $\mathbb{Z}_k$  Parafermion Quantum Hall Islands and Measurement of Non-Abelian Anyons,” *J. of Geom. and Symm. in Phys.* **62** (2021) 1–28.
- [28] W. Pan, J.-S. Xia, V. Shvarts, D. E. Adams, H. L. Störmer, D. C. Tsui, L. N. Pfeiffer, K. W. Baldwin, and K. W. West, “Exact quantization of the even-denominator fractional quantum Hall state at  $\nu = 5/2$  Landau level filling factor,” *Phys. Rev. Lett.* **83** (1999) 3530, cond-mat/9907356.
- [29] J. Xia, W. Pan, C. Vicente, E. Adams, N. Sullivan, H. Stormer, D. Tsui, L. Pfeiffer, K. Baldwin, and K. West, “Electron correlation in the second Landau level: a competition between many nearly degenerated quantum phases,” *Phys. Rev. Lett.* **93** (2004) 176809.
- [30] W. Pan, J. S. Xia, H. L. Stormer, D. C. Tsui, C. Vicente, E. D. Adams, N. S. Sullivan, L. N. Pfeiffer, K. W. Baldwin, and K. W. West, “Experimental studies of the fractional quantum Hall effect in the first excited Landau level,” *Phys. Rev.* **B 77** (Feb, 2008) 075307.
- [31] J. Fröhlich, U. M. Studer, and E. Thiran, “A classification of quantum Hall fluids,” *J. Stat. Phys.* **86** (1997) 821, cond-mat/9503113.
- [32] L. S. Georgiev, “Hilbert space decomposition for Coulomb blockade in Fabry–Pérot interferometers,” in *Lie Theory and Its Applications in Physics: IX International Workshop*, V. Dobrev, ed., Springer Proceedings in Mathematics & Statistics 36, pp. 439–450. 2011. arXiv:1112.5946. Proceedings of the 9-th International Workshop “Lie Theory and Its Applications in Physics”, 20-26 June 2011, Varna, Bulgaria.
- [33] L. S. Georgiev, “Thermopower and thermoelectric power factor of  $\mathbb{Z}_k$  parafermion quantum dots,” *Nucl. Phys.* **B 899** (2015) 289–311, arXiv:1505.02538.
- [34] A. Cappelli and G. R. Zemba, “Modular invariant partition functions in the quantum Hall effect,” *Nucl. Phys.* **B490** (1997) 595, hep-th/9605127.
- [35] L. S. Georgiev, “A universal conformal field theory approach to the chiral persistent currents in the mesoscopic fractional quantum Hall states,” *Nucl. Phys.* **B 707** (2005) 347–380, hep-th/0408052.

- [36] L. S. Georgiev, “Thermoelectric properties of Coulomb-blockaded fractional quantum Hall islands,” *Nucl. Phys.* **B 894** (2015) 284–306, arXiv:1406.6177.
- [37] S. Schweber, *An Introduction to Relativistic Quantum Field Theory*. Row, Peterson and Company, 1961.
- [38] H. Bateman and A. Erdelyi, *Higher Transcendental Functions*, vol. 1. McGraw-Hill, New York, 1953.
- [39] R. B. Laughlin, “Anomalous quantum Hall effect: An incompressible quantum fluid with fractionally charged excitations,” *Phys. Rev. Lett.* **50** (May, 1983) 1395–1398.
- [40] P. Bonderson, A. Kitaev, and K. Shtengel, “Detecting non-abelian statistics in the  $\nu = 5/2$  fractional quantum Hall state,” *Phys. Rev. Lett.* **96** (2006) 016803, cond-mat/0508616.
- [41] A. Stern and B. I. Halperin, “Proposed experiments to probe the non-Abelian  $\nu = 5/2$  quantum Hall state,” *Phys. Rev. Lett.* **96** (2006) 016802.
- [42] P. Bonderson, K. Shtengel, and J. K. Slingerland, “Probing non-abelian statistics with two-particle interferometry,” *Phys. Rev. Lett.* **97** (2006) 016401, cond-mat/0601242.
- [43] V. G. Knizhnik and A. B. Zamolodchikov, “Current Algebra and Wess–Zumino Model in Two Dimensions,” *Nucl. Phys.* **B 247** (1984) 83–103.
- [44] M. T. Rouabah, N. E. Belaloui, and A. Tounsi, “Compiling single-qubit braiding gate for Fibonacci anyons topological quantum computation,” *J. of Phys: Conference Series* **1766** (2021) 012029.